Spring 2019

Three-Dimensional Plasma Cell Survival Microniche in Multiple Myeloma

Katrina A. Harmon

THREE-DIMENSIONAL PLASMA CELL SURVIVAL MICRONICHE IN MULTIPLE MYELOMA

by

Katrina A. Harmon

Bachelor of Science
Winthrop University, 2014

Submitted in Partial Fulfillment of the Requirements

For the Degree of Doctor of Philosophy in

Biomedical Science

School of Medicine

University of South Carolina

2019

Accepted by:

Richard Goodwin, Major Professor

Jay Potts, Committee Member

Robert Price, Committee Member

Carole Oskeritzian, Committee Member

Sergio Arce, Committee Member

Cheryl L. Addy, Vice Provost and Dean of the Graduate School

DEDICATION

This dissertation took a great deal of time and energy, often at the expense of being with my loved ones. This dissertation is dedicated to them: to my mom, family, and dear friends for loving me unconditionally, for understanding, and for supporting me in pursuit of my aspirations.

You have been with me every step of the way, through the good times and bad. Thank you for all of the guidance and support that you have given me, helping me to succeed, and instilling in me the confidence that I am capable of doing anything I put my mind to.

Mom, I hope that through this work I am able to – in some way – repay you for all that you have sacrificed in order for me to become the woman that I am today. I assure you, greater is coming.

ACKNOWLEDGEMENTS

I would like to thank my advisor, Dr. Richard Goodwin, for his constant support and mentorship throughout my research endeavor. In addition, I would like to acknowledge the members of my committee, Drs. Jay Potts, Robert Price, Carole Oskeritzian, and Sergio Arce for their continuous encouragement and direction during my research. I would also like to thank current and former members of the Goodwin lab, Rebecca Jones and Sage Chang, for teaching me the “Goodwin way”. Thank you to my student assistants, Rachel Boone, Jane Goodwin, Matthew Kavolus, and Josh Muccitelli, for all of your help and daily laughs. In addition, I would like to acknowledge Dr. John Eberth and Brooks Lane for fostering me during my graduate career. I am greatly appreciative for your support.

Thank you to my collaborators, Dr. Suzanne Fanning and Sara Roman at Greenville Health System for providing patient samples and clinical guidance. I would also like to acknowledge Anna McNeal Harper for her encouragement and never-ending knowledge during this research. Furthermore, I would like to thank Drs. Heather Evans-Anderson and Erika Blanck and my PREP mentors, Drs. Bert Ely and Richard Hunt, for pushing me towards success from the very start. Thank you for seeing and fostering my academic potential.

ABSTRACT

Multiple myeloma (MM) is an incurable malignancy characterized by the uncontrolled proliferation of long-lived plasma cells (PCs) in the bone marrow (BM), which constitute at least 10% of BM cellularity. Normally, long-lived plasma cells make up less than 1% of BM cells. Plasma cells become neoplastic when a clonal PC population produces a monoclonal immunoglobulin protein. A diagnosis of monoclonal gammopathy of undetermined significance (MGUS) is made when there is an increase in monoclonal PCs within the BM, but less than 10%, and the patient does not present with end-organ damage, which is associated with active MM. Though not considered pathological at this stage, individuals with MGUS are at an increased risk for developing MM. There are several challenging aspects in treating MM including the high clonal heterogeneity of MM cells and its clinical repercussions, thus making the malignancy difficult to treat. Further heterogeneity is found in regard to disease onset, disease progression, therapeutic resistance, and subsequent patient relapse.

The purpose of this project is to investigate the microniche of PCs as they transition from premalignant to malignant myeloma cells in order to provide valuable insight which can be exploited to test current and novel therapeutic treatments. This project has demonstrated changes in the expression of fibronectin and morphological differences in plasma cells within core biopsies, which may support disease progression. Additionally, the purpose of this project is also to

generate a long-term 3D *in vitro* culture models of MM using a high-throughput hydrogel platform. By using BM aspirates from MGUS and MM patients, results demonstrated that this 3D culturing system is capable of reproducing key features on long-lived PCs. Furthermore, these BM cultures maintained their abnormal phenotypes for at least five days of culture. This extended timeframe allows for better characterization of the mechanisms of action of current therapies and testing of emerging treatments for this incurable disease.

TABLE OF CONTENTS

LIST OF FIGURES

LIST OF ABBREVIATIONS

APRIL ..... A proliferation-inducing ligand

BCMA ..... B-cell maturation antigen

BM ..... Bone marrow

BMSC ..... Bone marrow stromal cell

ER ..... Endoplasmic reticulum

ECM ..... Extracellular matrix

Ig ..... Immunoglobulin

IL-6 ..... Interleukin 6

LC3 ..... Microtubule-associated proteins 1A/1B light chain 3B

MGUS ..... Monoclonal gammopathy of undetermined significance

MM ..... Multiple myeloma

Mcl-1 ..... Myeloid cell leukemia-1

PC ..... Plasma cell

UPR ..... Unfolded protein response

VLA-4 ..... Very late antigen 4

CHAPTER 1

INTRODUCTION

Multiple myeloma (MM) is an incurable hematological cancer caused by the uncontrolled proliferation and expansion of plasma cells (PCs) within the bone marrow (BM). This second most common hematologic malignancy is associated with progressive immune dysregulation characterized by decreased antigen-presenting and effector cell function, loss of myeloma-reactive T lymphocyte populations, and a BM microenvironment that promotes immune privilege. In 2019, it is estimated that there will be 32,110 new cases of MM with approximately 12,960 deaths.[1] The exact cause of MM is unknown and no avoidable risk factors have been found. MM is more common in individuals over age 65. Furthermore, men are slightly more likely to develop MM and individuals of African American descent are twice as likely to develop the disease.[1,2] Additionally, individuals with other PC diseases, such as monoclonal gammopathy of undetermined significance (MGUS) or a single tumor of PCs, are at a higher risk of developing MM. Once diagnosed, a limited number of treatment options are available for patients, though MM can be controlled in most patients, sometimes for many years. Without treatment, the median survival rate is typically less than seven months, but treatment extends survival to four to five years, with a five-year survival rate of 49%. Despite novel therapeutic advancements, MM still remains an incurable neoplasia due to intrinsic or acquired resistance to therapy.[3]

1.1 Plasma Cell Development

Plasma cells are terminally differentiated, non-dividing effector cells of the B lymphocyte lineage. These cells are devoted to synthesizing and secreting immunoglobulins (Igs), leading to a range of specificity of both lambda and kappa light chains.[4,5] To respond to microbial pathogens with specificity and rapidity, B lymphocytes are regulated by their development in the BM and subsequent activation in the periphery. PCs are maintained for extended periods allowing for potential life-long immunity to pathogens, which constitutes a crucial component of humoral immune memory.[6] Though PCs are recognized as the basis of humoral immunity, the complexities of PC development have made it apparent that not all PCs are the same. They differ in lifespan, localization, and the expression of cell surface markers and transcription factors associated with PC fate and immunoglobulin secretion.[7,8]

PCs can become neoplastic when a clonal PC population produces a monoclonal immunoglobulin protein, such as all IgG kappa or IgG lambda, and this abnormal paraprotein can be detected in the blood and urine. In general, when plasma cells become malignant and proliferate uncontrollably, this is diagnosed as MM.

1.2 Characterization of Multiple Myeloma

Cancerous PCs, constituting ≥10% monoclonal PCs, can cause end-organ damage including calcium (elevated), renal insufficiency, anemia, and bone

lesions (C.R.A.B), thereby meeting criteria for active MM.[9–11] The usual balance between bone resorption and new bone formation is lost in MM, resulting in bone destruction. Osteoclasts are increasingly prominent in the BM microenvironment because of their activation by various cytokines and signaling pathways. The excessive resorption by osteoclasts overpowers the protective effects of osteoblasts, resulting in a cycle that ongoingly releases calcium in the blood leading to hypercalcemia.[12–14] Hypercalcemia can cause a variety of symptoms for patients including excessive thirst, nausea, constipation, loss of appetite, and confusion.

Renal failure in MM patients is most commonly due to the excessive production of immunoglobulins by the myeloma cells. Depending on the size of these abnormal paraproteins, they may be excreted through the kidneys, which can cause damage. Additionally, hypercalcemia further contributes to renal failure in patients.[15]

Anemia is present in 73% of patients at the presentation of the disease and in 97% of patients during the course of the disease. This is caused by the replacement of normal BM being infiltrated by malignant myeloma cells, leading to the inhibition of normal red blood cell production.[9]

In the majority of myeloma patients, hypercalcemia can also cause bone lesions and bone pain. Bone destruction develops adjacent to myeloma cells, yet not in areas of normal BM.[13] When more than 30% of the bone has been destroyed, X-rays show a thinning of the bone (osteoporosis) or lytic lesions and these weakened areas of bone are more likely to facture. Most patients experience bone

pain, especially in the middle and/or lower back, rib cage, hips, or spine. Bone fractures and spinal cord compression are the most common.[11] This pain may be mild or severe depending on the extent of the myeloma, the speed with which it has developed, and whether a fracture or nerve compression has occurred.

There are other neoplastic plasma cell disorders that have abnormal PCs, but do not meet the criteria to be classified as active MM. Monoclonal gammopathy of undetermined significance (MGUS) is a precancerous condition and the most common hematological malignancy capable of producing monoclonal plasma cells.[16,17] MGUS resembles MM, but the levels of antibodies are lower, the number of PCs in the BM is lower (less than 10%), and patients do not present with end-organ damage.[14,18] MGUS patients rarely have symptoms or major problems, however these patients can progress to MM at an average rate of ~1% per year.[17,19,20] As a result, most patients never develop a PC malignancy and because of this MGUS has gained a relatively benign reputation. Unfortunately, this is not accurate as recently it has been recognized that nearly all cases of MM are preceded by a period of MGUS.[19]

1.3 Bone Marrow Microenvironment

The BM microenvironment consists of cellular and non-cellular compartments.[12,21–24] The cellular compartment can be subdivided into hematopoietic cell types including myeloid cells, T lymphocytes, B lymphocytes, natural killer cells, and osteoclasts, while non-hematopoietic cells include bone marrow stromal cells (BMSCs)/fibroblasts, osteoblasts, and endothelial cells, in

addition to blood vessels.[25] The non-cellular compartment of the BM includes a complex extracellular matrix (ECM), oxygen, and a liquid milieu composed of cytokines, growth factors, and chemokines, which are produced by the cellular compartment within the BM microenvironment. The BM ECM consists of fibronectin (FN), laminin, proteoglycans, glycosaminoglycans, and various collagens, which provide scaffolding for the cellular compartments. ECM arrangement is critical for normal hematopoiesis and the tumor microenvironment of various cancers by contributing to cell survival, proliferation, and metastasis.[26,27]

1.4 Plasma Cell Niche

The fundamental observation that plasma cells are sustained within the BM for decades implies that BM provides a complement of survival factors that support their existence. Once established within a BM niche, plasma cells can persist, effectively becoming long-lived PCs. Numerous factors, both soluble and insoluble, have been described to contribute to the long-lived PC niche.[28,29] PCs also require specific cell-cell interactions with BM stromal cells to persist. This interaction induces stromal cell production of interleukin-6 (IL-6), which enhances plasma cell survival.[29,30]

Unlike normal PCs which migrate throughout peripheral tissues, long-lived PCs reside within the BM and slowly proliferate. It is thought that BM resident long-lived PCs are transformed into MM cells with the ability to uncontrollably proliferate. Myeloma cell localization within the BM milieu allows for cell-cell interactions between tumor cells and non-tumor BM cells, which promote neoplastic cell

growth, survival, bone disease, acquisition of drug resistance, and consequential relapse.[3,31] Additionally, research has shown that interactions between PCs and ECM within this niche contributes to myeloma cell survival and therapeutic resistance.[22,32]

Soluble and membrane-bound survival factors found in normal long-lived PC niches, such as IL-6, have been shown to play a critical role in promoting plasma cell activity in MM. Additional factors such as A Proliferation-Inducing Ligand (APRIL) and myeloid cell leukemia-1 (Mcl-1) are also important in the survival of myeloma cells.[28] These essential survival factors play a role in maintaining the growth and expansion of plasma cells within the BM.[33] Several survival ligand–receptor pairs have been discovered both *in vitro* and *in vivo* including: FN–very late antigen 4 (VLA-4), IL-6–gp130, and APRIL–B-cell maturation antigen (BCMA).[34] Specifically, IL-6 is emphasized as a key player in MM pathogenesis by inhibiting apoptosis in myeloma cells. IL-6 also interacts with several factors involved in the development and progression of MM, such as adhesion molecules, tumor suppressor genes, and oncogenes.[35,36] Clinically, MM patients have elevated serum levels of IL-6, which is associated with poor prognosis.[37] APRIL is also necessary for the survival of PCs and, when bound to BCMA, can activate several signaling pathways that mediate cell growth and survival.[38–41] Mcl-1 is similarly critical for the survival of myeloma cells *in vitro* and *in vivo*.[42] Through its overexpression in myeloma cells, Mcl-1 contributes to therapeutic resistance in conventional chemotherapies.[43–45] Furthermore, Mcl-1 is

highly regulated by survival signaling triggered by various cytokines and growth factors located in the BM liquid milieu.

1.5 Treatment of Multiple Myeloma

It is known that the PC niche and surrounding BM microenvironment play significant roles in supporting the growth, survival, progression, and therapeutic resistance in MM, thereby representing an ideal target for anti-MM therapies. For more than the past 15 years, new classes of nongenotoxic treatments disrupting the interactions between myeloma cells and its niche have been introduced into the therapeutic armamentarium for MM. This has led to substantial improvements in the treatment of this disease. In particular, the immunomodulatory drugs thalidomide and lenalidomide, and the first-in-its-class proteasome inhibitor bortezomib, have formed the backbone of newer treatments that are currently used in both up-front and relapse-refractory settings.[46–48] Additionally, the more conventional treatment option of glucocorticoids, such as dexamethasone, remains widely used in combination therapies with immunomodulatory drugs and proteasome inhibitors.[26] Stem cell transplantation, allogeneic and autologous, is also a treatment option for select myeloma patients. Autologous stem cell transplantation is more common, where the patient's own hematopoietic stems cells are infused back into the patient's blood after treatment with high-dose chemotherapy or radiation.[49] Despite the increasing therapeutic advancements that prolong patient survival, MM remains an incurable malignancy.[48] Nearly all patients eventually relapse, and this high rate of relapse, which is sometimes

refractory, suggests that more effective and sensitive treatment methods remain imperative.

1.6 Current Approaches

Novel approaches used to treat MM focus on disruption of the myeloma cell microenvironment, which provides numerous essential survival factors and scaffolding that allows for the persistence of malignant PCs. Though this niche has been defined biochemically and genetically, the 3D microstructure has not been clearly resolved.[25] Research demonstrates that normal and malignant plasma cell niches differ in gene expression profiles, cell phenotypes, and function. Thus, the 3D arrangement of the BM ECM and survival factors are likely to differ in normal and malignant states. Numerous hurdles are present in studying human PCs.

There is a lack of *in vitro* systems available to generate and maintain mature long-lived PCs. The vast majority of *in vitro* research using myeloma cells have been carried out in 2D or planar cultures; however, PC *in vitro* survival is short and variable with no indication of an extended life span.[50] Additionally, preclinical studies using simplistic *in vitro* models have found novel anti-MM agents that have not translated to *in vivo* clinical benefits. This is due to the lack of studies on 3D BM architecture and/or tumor microenvironment, which are necessary to adequately model the disease and limited studies have utilized 3D culture techniques.[51–55]

1.7 Rationale

The overall goal of this project is to investigate differences in the BM microenvironment of patients being screened for MGUS and MM, while also generating a patient specific collagen-based three-dimensional *in vitro* model of the disease. This would allow for the investigation of the complex interactions which occurs as the BM transition from premalignant to active MM. There are biochemical and genetic changes between normal and malignant plasma cell niches. Therefore, investigating microstructural differences between the premalignant and malignant stages can provide valuable information that can be exploited to test current therapies, as well as the development of novel treatments.

The overall hypothesis of this study is that changes in the 3D microenvironment of premalignant and malignant plasma cells promote oncogenesis and therapeutic resistance. The results described herein stem from specific aims designed to examine factors influencing plasma cells in the BM microniche of MM patients:

Specific Aim 1: To elucidate differences in the microenvironment of premalignant and malignant plasma cells.

Specific Aim 2: To generate a 3D patient specific *in vitro* model of multiple myeloma malignant transformation and resistance.

CHAPTER 2

BONE MARROW MICROENVIRONMENT AND PLASMA CELL NICHE OF MULTIPLE MYELOMA PATIENTS

2.1 Abstract

Multiple myeloma is a hematologic malignancy that is characterized by the proliferation of abnormal bone marrow plasma cells and the overproduction of immunoglobulin with evidence of end-organ damage including hypercalcemia, anemia, renal dysfunction, and lytic bone lesions. The pathogenesis of MM is closely related to changes in the extracellular matrix, as well as the dysregulation of the unfolded protein response and ER stress. This study revealed significant changes in fibronectin expression, which was associated with disease progression. Additionally, electron micrographs of plasma cells from BM biopsies exhibited morphological changes from the transition of monoclonal gammopathy of undetermined significance to active multiple myeloma. Furthermore, the presence of LC3 puncta in myeloma patients represent the presence of autophagy within patient samples.

2.2 Introduction

Despite the introduction of new targeted treatments, multiple myeloma (MM) remains an incurable plasma cell (PC) neoplasm.[12,25,56–58] It is the second most common hematologic malignancy, accounting for 10% of all hematological malignancies.[49] In 2019, it is estimated that there will be 32,110 new cases of MM with approximately 12,960 deaths.[1] MM is a cytogenetically heterogenous clonal disorder that typically evolves from an asymptomatic premalignant stage called monoclonal gammopathy of undetermined significance (MGUS) prior to becoming active, symptomatic MM.[11,15,19]

Endoplasmic Reticulum Stress, Unfolded Protein Response, and Autophagy in Multiple Myeloma

One of the characteristics of MM is the excessive production of monoclonal immunoglobulin, also referred to as paraprotein, by malignant PCs. This high level of immunoglobulin production induces endoplasmic reticulum (ER) stress and proteasomal degradation of the paraprotein is required to avoid ER stress-induced apoptosis.[59,60] ER stress occurs when there is an accumulation of unfolded and/or misfolded protein which exceeds the rate of protein refolding or degradation. With an exception of a small subset of patients (1-5% of MM patients), most patients diagnosed with MM characteristically produce excessive levels of paraprotein.[60,61] The continual production of paraprotein subjects myeloma cells to continual ER stress allowing for myeloma cells to become highly dependent on the unfolded protein response (UPR) for survival.[59]

Myeloma cells exploit several molecular mechanisms to counteract the toxic proteins including UPR pathway, the upregulated expression of heat shock protein chaperones, and the autophagy-lysosome pathway.[62–64] Increased UPR mediated signaling can coordinate and activate autophagy to reduce ER stress.[65,66] Consequently, the induction of ER stress mediates apoptosis in myeloma cells, increasing survival. The pathogenesis of MM is closely linked to dysregulation of the UPR in the ER.[67,68] Studies have shown that key downstream chaperones, such as grp94, in the ER that mediates the UPR is highly expressed in malignant plasma cells in patients with MM, but not in patients with MGUS.[68]

Autophagy offers a potential pathway that may protect myeloma cells as it is crucial for sustainable immunoglobulin production by plasma cells and for the long-lived humoral immunity.[63] Autophagy is a degradation process of proteins and organelles in which double-membrane vesicles, called autophagosomes, sequester cytosolic proteins and/or organelles. Studies suggest that autophagy may be a critical additional process by which the malignant PCs could protect from toxic misfolded immunoglobulins.[69] Limited studies have demonstrated changes in autophagy with the disease progression of MM.

Bone Marrow Microenvironment in Multiple Myeloma

The current treatment approach for MM includes immunomodulators, proteasome inhibitors, glucocorticoids, and autologous hematopoietic stem cell transplantation.[9,56] Though these treatments target the BM microenvironment and prolong the survival of MM patients, MM remains an incurable disease and nearly

all patients eventually relapse. High rates in relapse suggest that clinically undetectable minimal residual disease persists after treatment, and proliferation of the remaining myeloma cells cause the ultimate relapse.[27] This indicates the importance of the BM microenvironment for malignant progression. The bone marrow (BM) tissue is thought to contain at least four types of extracellular matrix (ECM) proteins, including fibronectin (FN), which is expressed throughout the BM.[70] The expression and activation of adhesion molecules, such as FN, are essential for mediating homotypic interactions among nearby myeloma cells and the heterotypic engagement by surrounding BM stromal cells.[21] This increased expression is essential for the development of chemotherapeutic drug resistance in MM patients.[71] Therefore, the discovery of more effective and selective therapies remains imperative. The effects of autophagy on the survival of myeloma cell and changes in the fibronectin may provide critical insights for the treatment of the disease.

The biochemical and genetic composition of normal and malignant plasma cells have been studied, yet limited research is available that examines possible 3D microstructural differences and its relationship to myeloma cell survival and therapeutic resistance.[6,72–74] Thus, examining the 3D microniche of MM patient biopsies can elucidate changes in the microniche of premalignant and malignant plasma cells. Here, microscopy techniques were utilized to examine differences in fibronectin and autophagy in the plasma cell niche of MM patients.

2.3 Materials and Methods

Patient Biopsy Samples

Bone marrow core biopsies were obtained from patients undergoing diagnosis for MGUS, low MM (10-20%), and high MM (>20%). Approval for these studies was obtained from Greenville Health System Institutional Review Board and all patient samples were collected after informed consent per GCP guidelines (IRB # Pro00067642). After patient biopsy, BM cores were immediately place into 4% paraformaldehyde or 2%gluteraldehye/2% paraformaldehyde for confocal microscopy and transmission electron microscopy, respectively.

Immunofluorescence

Bone marrow core samples fixed in 4% paraformaldehyde for immunofluorescence were extensively washed in 1X phosphate-buffered saline (PBS) to remove excess fixative prior to staining for CD138, a plasma cell marker (no.PA5-16918; Thermo Fisher, Waltham, MA USA), fibronectin (no. MAB19181; Novus, Centennial, CO USA), and LC3, an autophagy marker (no. GTX632501; GeneTex, Irvine, CA USA). Samples were decalcified using 14% ethylenediaminetetraacetic acid (EDTA) in ammonium hydroxide at room temperature, with daily changes of the 14% EDTA solution (~2 – 4 days), prior rinsing in PBS two times for 1 hour each. Samples were soaked in 15% sucrose in PBS at 4ºC with constant agitation until sample sinks to bottom then immersed in 30% sucrose in PBS at 4ºC with constant agitation overnight. Samples were then embedded in Tissue Plus O.C.T. Compound. Samples were frozen rapidly using

dry ice and 2-methyl-butane. The frozen samples were sectioned at 10-20 μm using the Zeiss Microm 505HN Cryostat.

Non-decalcified core biopsies were permeabilized with 0.1% Triton X-100/PBS three times for 30 min each followed by a 0.3M Glycine wash for 45 min and three rinses in PBS. Samples were then blocked in 5% bovine serum albumin in phosphate-buffered saline (BSA/PBS) for one hour at room temperature before being placed in 2%BSA/PBS overnight at 4°C with constant agitation. Samples were incubated in primary antibodies [1:100] in 1%BSA/PBS for two days at 4°C. BM cores were rinsed with 1%BSA/PBS three times for 20 min each prior to incubating with secondary antibodies [1:100] in 1%BSA/PBS for two days at 4°C (Alexa 488 and Alexa 546 no. A11034, no. A11003, Thermo Fisher, Waltham, MA USA; DyLight 550 no. NB7494R Novus, Centennial, CO USA). Biopsies were rinsed two times for 20 min each in PBS prior to being counterstained with DAPI [1:5000] for 40 min at room temperature. Samples were then rinsed with PBS for 20 min prior to mounting with deionized water. Images were captured on the Lecia SP8 multiphoton confocal.

Decalcified, frozen sections were permeabilized with 0.1% Triton X-100/PBS, washed in 0.3M Glycine, and blocked with 2% BSA/PBS buffer as previously stated. Sections were incubated in primary antibodies [1:100] overnight at 4ºC then secondary antibodies [1:100] were incubated for 1 hour at 37ºC prior to rinsing and counterstaining with DAPI [1:5000]. Sections were mounted with DABCO and imaged using Lecia SP8 multiphoton confocal and Lecia SP8 TCS confocal microscope.

The percentage of area occupied by fibronectin was quantified by randomly selecting three imaging areas within a patient BM for MGUS (n=3) and MM (n=3) patients. The average percentage was calculated.

Transmission Electron Microscopy (TEM)

Approximately 1mm^3 of the fresh core biopsy was immediately fixed in 2% glutaraldehyde/2% paraformaldehyde under constant agitation at 4°C. Samples were decalcified using 14% EDTA solution. Samples were rinsed three times in 1X PBS buffer for 30 min each at room temperature. A secondary fix in an OsO_4 solution (1% osmium tetroxide with 1.5% K+ Ferricyanide) was done for 30 min. Samples were quickly rinsed with water then rinsed again with water twice for 10min each. The sample was dehydrated in an ethanol gradient of increasing concentrations: 70% ethanol twice for ten min each, 95% ethanol twice for ten min each, and lastly 100% ethanol twice for ten min each. Next, the sample was changed to the intermediate solvents: 1:1 ratio of ethanol to acetonitrile for five min, and then in 100% acetonitrile twice for ten min each. To prepare the resin, PolyBed 812 was removed from the freezer, previously prepared. Briefly, the resin was prepared accordingly: 51.13 g of PolyBed812, add DDSA until 78.15g, add NMA until 100.00g. The resin solution was mixed well, including the sides, and stored in 50mL conicals at -20□C until ready for use. The resin was warmed to room temperature followed by the addition of 0.4mL DMP-30. The mixture was stirred, not vortexed, thoroughly before proceeding. For resin infiltration, a 2:1 ratio of acetonitrile to PolyBed 812 was added to the sample for 30 min followed by the

addition of a 1:2 ratio of acetonitrile to PolyBed 812 for 30 min. Pure PolyBed 812 was added twice, the first for 30 min and the second overnight on the rotator.

Sample embedding was completed on the second day. One piece of tissue was added in each Flat Embedding Mold before filling the mold to the top with PolyBed 812. After the molds were labeled, they were placed into a 60ºC oven for 48 hours.

Samples were sectioned ultrathin at a thickness of 100nm, which were subsequently stained with 2% uranyl acetate and Hanaichi lead citrate. Images were captured with the JEOL 1400 Plus Transmission Electron Microscope.

Statistical Analysis

Statistical analysis to evaluate changes in percentage of area occupied by fibronectin was determined by an unpaired t test. Data are reported as mean ± SD. Differences between groups were considered significant at $P < 0.05$.

2.4 Results

Changes in Fibronectin Associated with Disease Progression

Frozen BM core sections were stained and imaged to determine changes in FN expression associated with disease transition from MGUS to active MM. Data demonstrated that MGUS patients presented with a low percentage of fibronectin expression, based on staining intensity (Figure 2.1), and there is minimal plasma cell involvement. As the disease progressed to active MM, patient

cores displayed a significant increase in the percentage of fibronectin expression associated with the increase of CD138+ cells (Figures 2.2, 2.3, 2.4).

Plasma Cell Morphology and Autophagy

Bone marrow biopsies from patients being screened for premalignant MGUS and malignant MM were subjected to transmission electron microscopy to demonstrate differences in plasma cell morphology as it relates to disease progression. Plasma cells from these core biopsies were found to have eccentric nuclei (Figures 2.5A, 2.6A, 2.6A), typical of normal PC morphology. In addition to these normal PCs, MGUS, low MM, and high MM samples were observed to have atypical plasma cells with extensive ER found throughout their cytoplasm (Figures 2.5B, 2.6B, 2.7B). Additionally, a third phenotype of PC was observed in MM patients. These PCs were found to have densely packed vesicles throughout their cytoplasm (Figures 2.6C, 2.7C), which was not seen in the premalignant core samples. This phenotype is indicative of a cell undergoing autophagy.[65]

To delineate the presence of autophagy in myeloma patient samples, core biopsies were stained with CD138 and LC3, an autophagosome marker. MGUS and myeloma patients exhibited areas of diffuse distribution of the LC3 protein, while other areas within the same sample presented with punctuated patterns of LC3 (Figure 2.8).

2.5 Discussion

Changes in the BM microenvironment and plasma cell niche contribute to the disease progression and persistence of MM. The ECM arrangement plays a crucial role in normal hematopoiesis and the tumor environment of various cancers by contributing to cell survival, proliferation, and metastasis.[13,27,75] The homing of myeloma cells to the BM depends on their interaction with ECM proteins, as well as autocrine and/or paracrine signaling mediated by chemokines and growth factors. Collagen type I, collagen type IV, fibronectin, and laminin are critical ECM proteins present within the BM, with collagen type I and fibronectin predominating.[34,76] Integrins mediate the binding of myeloma cells to ECM molecules and research has shown that myeloma cells strongly adhere to fibronectin.[77] Additionally, the interactions between PCs and ECM can contribute to myeloma cell survival and therapeutic resistance.[22,32] In this study, there was a significant increase in percentage of area occupied by fibronectin as the disease progressed from MGUS to MM. The increase in FN expression was associated with increases in CD138+ plasma cells. Thus, further supporting the view that FN plays a key role in the tumor microenvironment of MM.

Multiple myeloma is a heterogenous entity with variable course and plasma cells within the BM have a high diversity of morphology. Studies focusing on BM smears have determined that some morphological features are more common in clinically advanced disease, such as the number of nucleoli, the number of myeloma cells with irregular nuclei, and larger nuclei. [78–80] In this study, electron

micrographs displayed differences in plasma cell morphology that relates to disease progression. Plasma cells within the samples have eccentric nuclei, which is morphologically associated with normal PCs. Extensive rough ER was found throughout the cytoplasm of plasma cells for all patient groups (MGUS, low MM, high MM). This is in contrast to normal PCs that have little to no observable ER. The abundant amount of ER may be due to increases in ER stress due to the production of monoclonal immunoglobulin, which allows myeloma cells to become dependent upon the UPR as a key mechanism for malignant PC survival.[59] Electron micrographs from MM patients also exhibited ab increase in densely packed vesicles, which was not present within MGUS samples. These results warrant further investigation to determine if autophagosomes were present within the BM cores.

The excessive production of monoclonal immunoglobulin relies on the UPR for myeloma cell survival. [60,64] Studies have found that the UPR can trigger autophagic activation in response to the accumulation of unfolded proteins. Studies have also shown that autophagy may be an important additional process by which malignant plasma cells could be protected from the toxic misfolded paraprotein.[69,81,82] Furthermore, basal autophagy levels have been found in myeloma cells as a response to ER stress, and the activation of autophagy has been shown to be important for myeloma cell viability.[65] Results from this study have demonstrated LC3 punctate staining within MGUS and MM patient core samples, which is indicative of autophagosomes. Additionally, areas presented with diffuse LC3 staining, suggesting that autophagosomes are not present

throughout the entire BM core. These results would further support that view that autophagy is ramped up in transformed cells, but not in normal plasma cell niches, and that this increase is beneficial for tumor maintenance and progression.[83,84]

2.6 Conclusions

In this study, premalignant and malignant patient BM cores displayed changes in fibronectin expression and plasma cell morphology. MGUS and myeloma patients also exhibited with LC3 puncta, which is associated with autophagy. These results elucidated changes in the BM microenvironment that play critical roles in the survival and progression of myeloma cells, further demonstrating the importance of the PC niche. Ultimately, these results can provide insight into 3D microstructural differences, which may be ideal targets for the therapeutic treatment of MM.

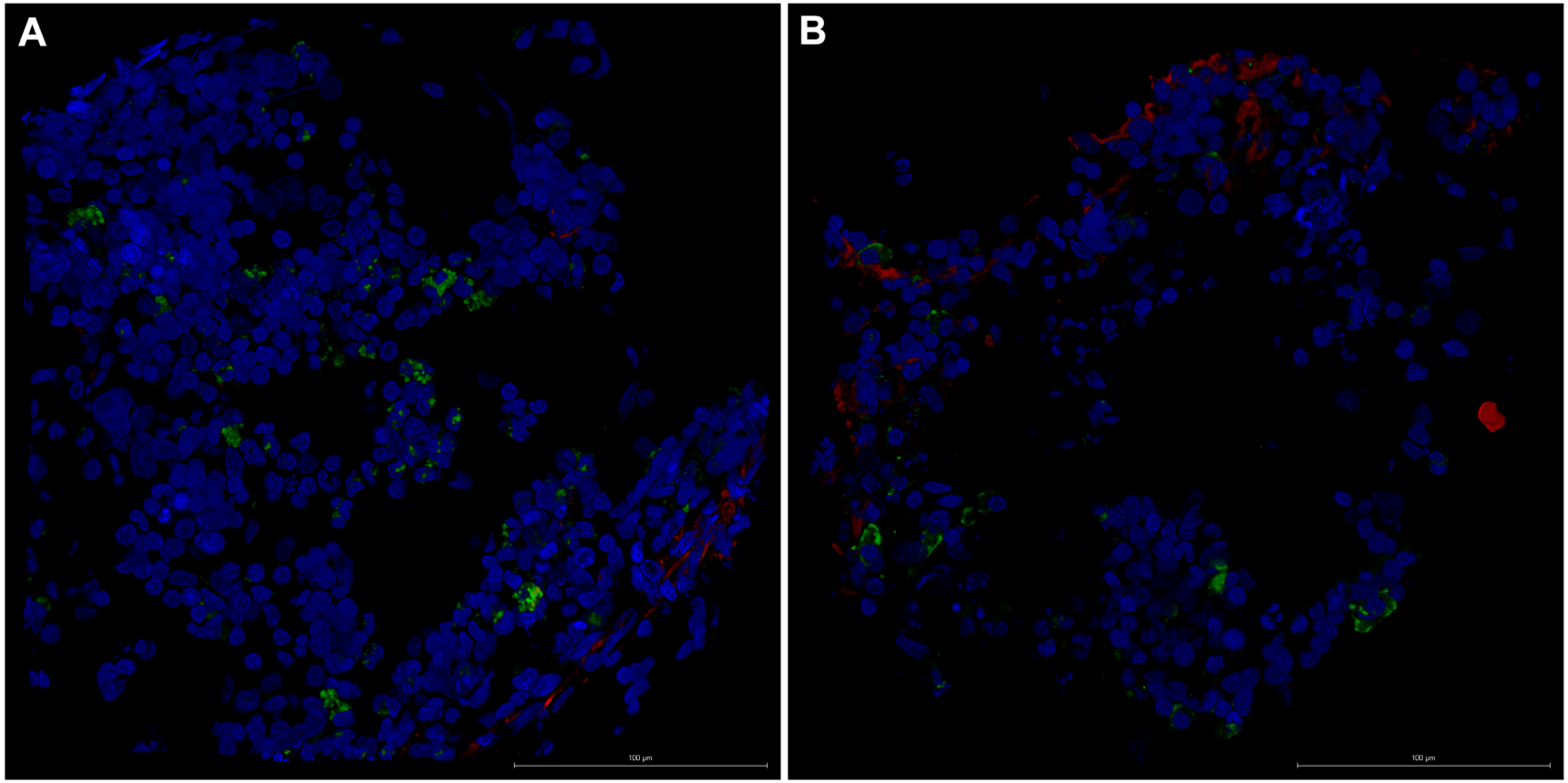

Figure 2.1. Representative confocal images from two MGUS bone marrow core cryosections exhibited less than 10% plasma cells (green) with low expression levels of fibronectin (red) staining intensity. Blue staining is DAPI. Scale Bars: 100µm.

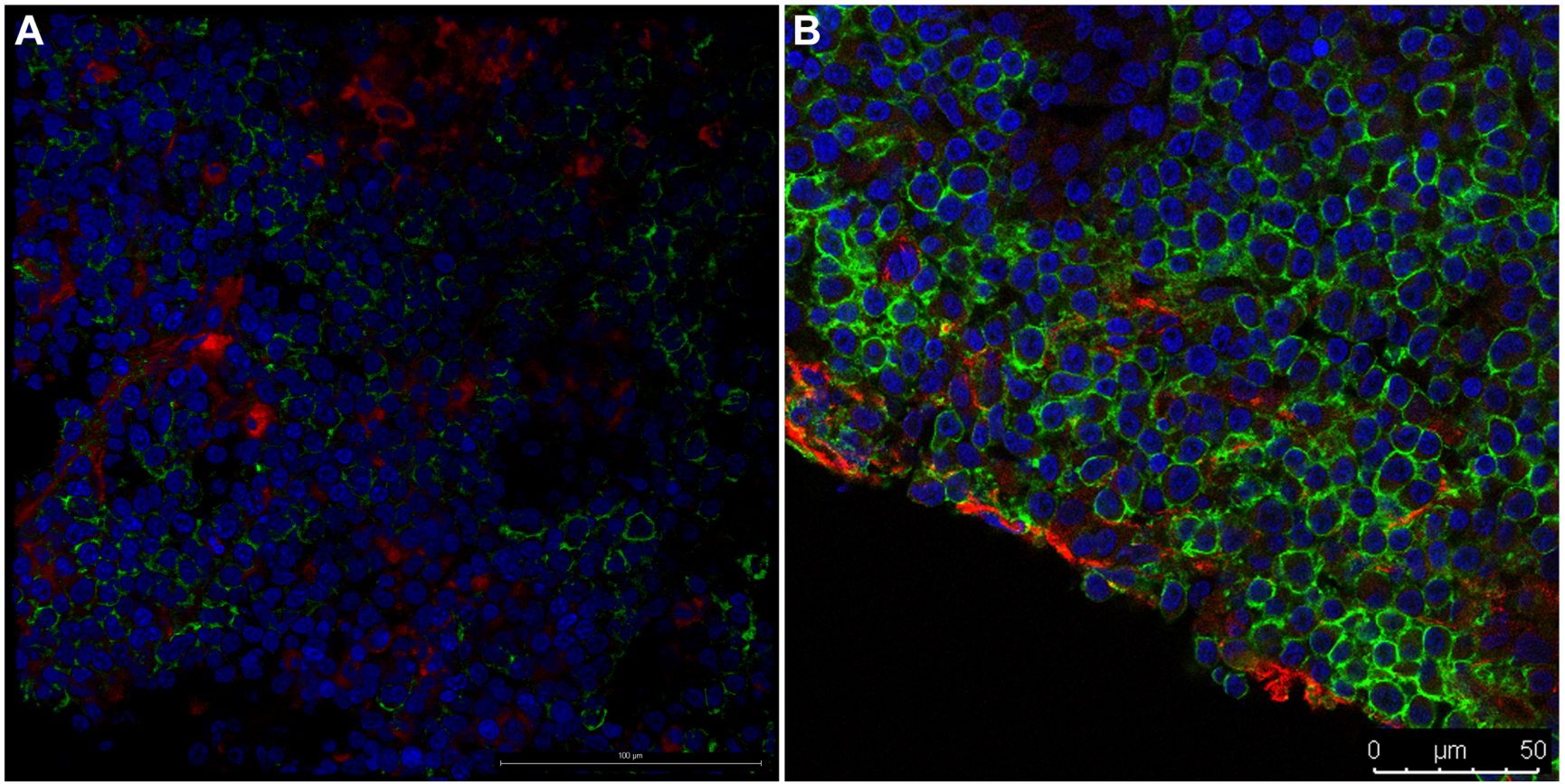

Figure 2.2. At low (A) and high (B) magnification, cryosectioned bone marrow cores from multiple myeloma patients display an increase in fibronectin expressed, based on staining intensity. Staining: DAPI (blue), CD138 (green), and FN (Red). Scale bars: 100µm and 50µm.

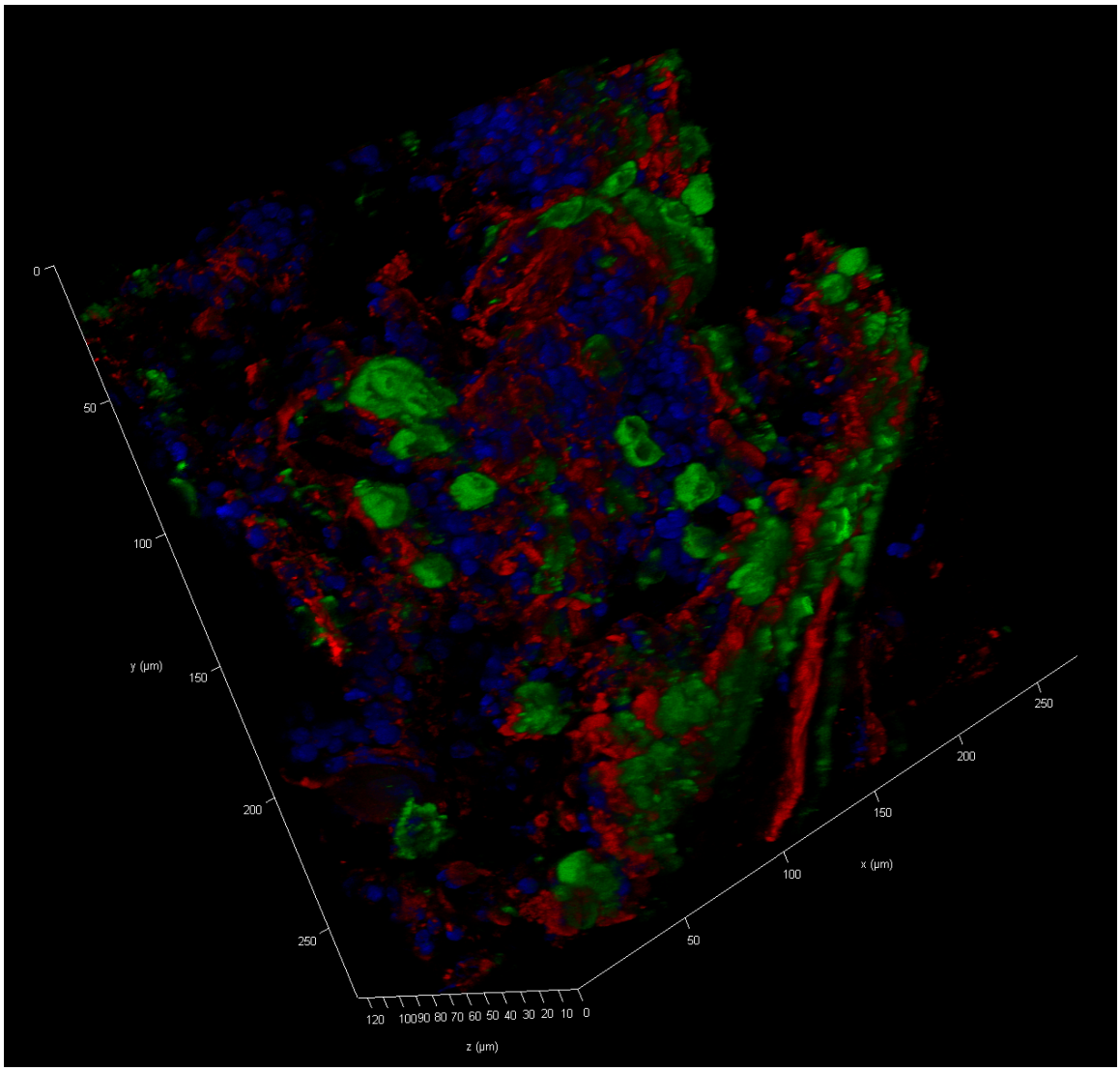

Figure 2.3. Non-decalcified myeloma bone marrow cores were stained for confocal microscopy, and the resulting Z-stack (120 µm) demonstrates increased fibronectin (red) expression that is associated with malignant, CD138+ plasma cells (green). Blue staining is DAPI.

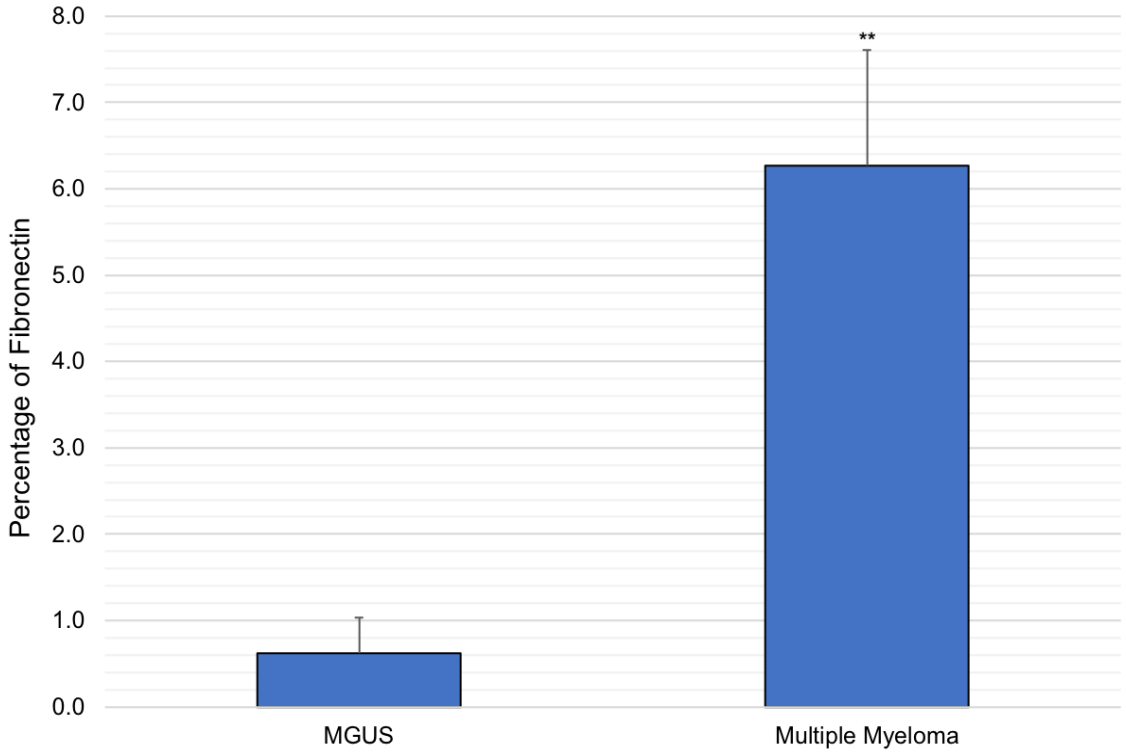

Figure 2.4. There is a significant increase in the percentage of fibronectin expression from the transition of MGUS to multiple myeloma. ** P ≤ 0.01.

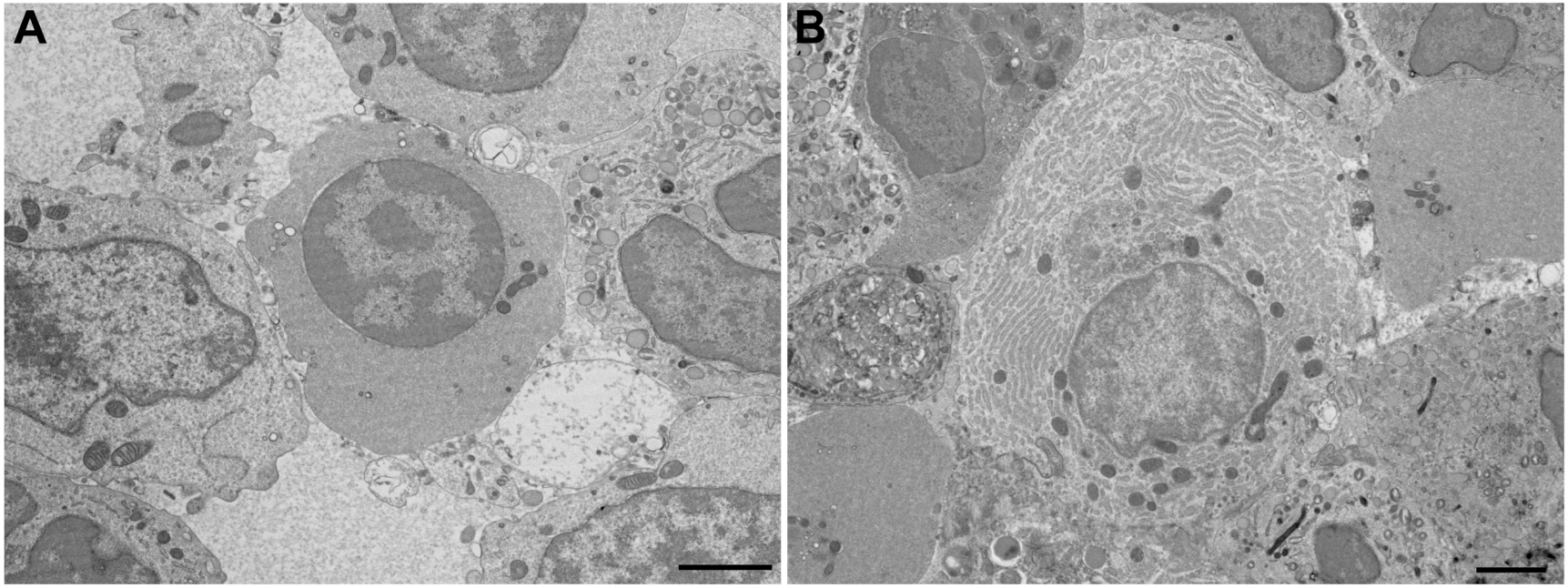

Figure 2.5. Representative electron micrograph of plasma cells from patients diagnosed with MGUS. Plasma cells (A) present with an eccentric nucleus, while other plasma cells within the sample present with an abundant amount of endoplasmic reticulum with minimal vesicles present (B). Scale bars: 2 μm.

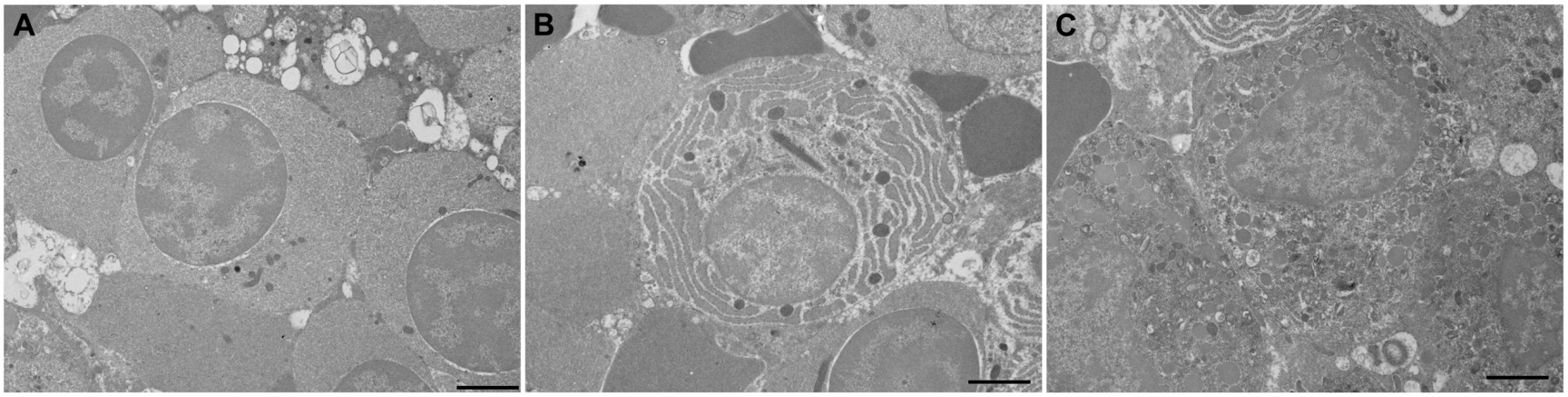

Figure 2.6. Electron micrographs of plasma cells from multiple myeloma patients with 10-20% monoclonal plasma cells. Differences can be seen between these plasma cells including increases in ER (B) and vesiculation (C). Scale bars: 2 μm.

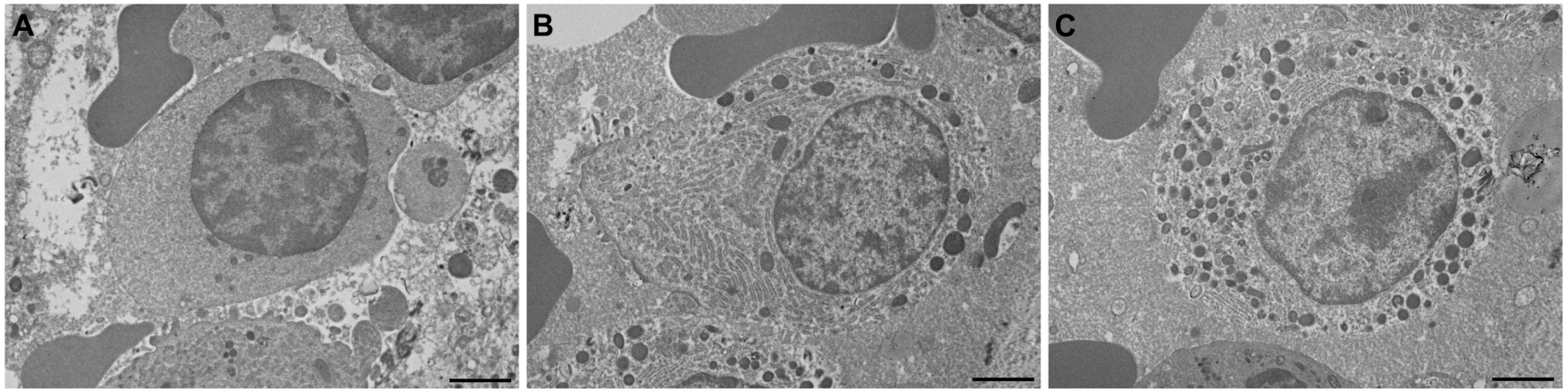

Figure 2.7. Electron micrographs from myeloma patients with <20% plasma cells present with normal eccentric nuclei (A), increases in ER (B), and increases in vesiculation (C). Scale bars: 2 μm.

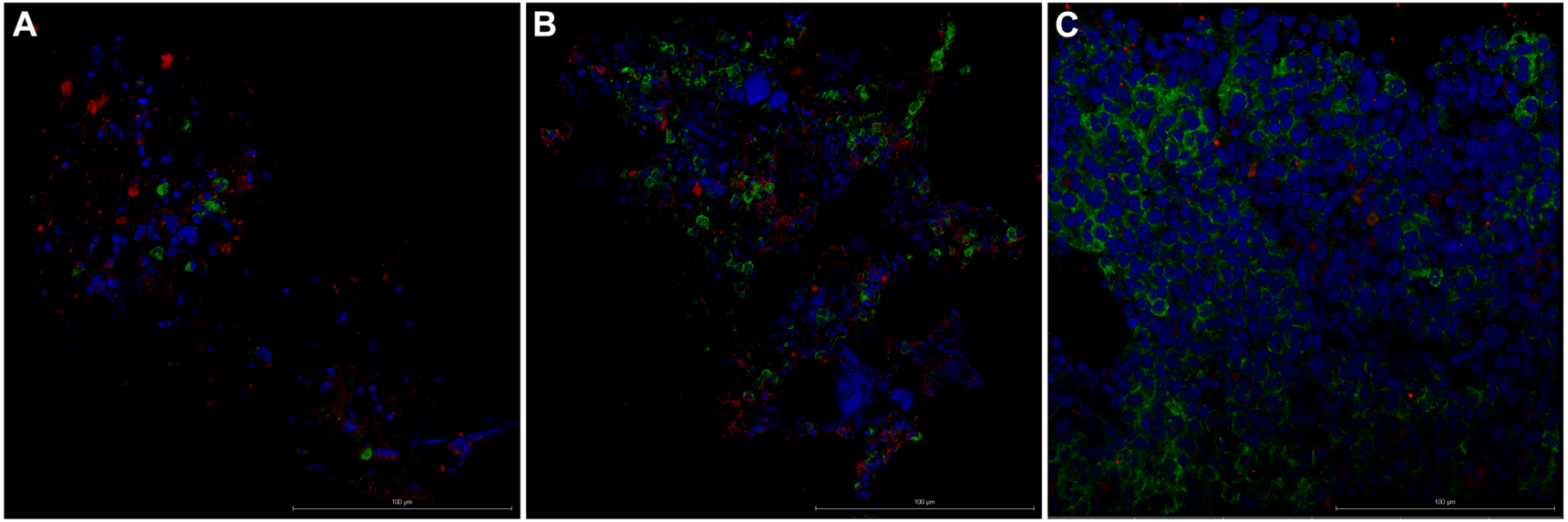

Figure 2.8. Non-decalcified BM cores for MGUS (A) and MM (B) patients, in addition to cryosections (C) from myeloma patients. Biopsies presented with both diffuse distribution and punctate pattern of LC3 protein (red). Blue staining is DAPI and green staining is CD138.

CHAPTER 3

PATIENT DERIVED THREE-DIMENSIONAL COLLAGEN MODELS OF MULTIPLE MYELOMA PROGRESSION

3.1 Abstract

Niches within the tumor bone marrow microenvironment create a unique milieu for multiple myeloma cells due to interactions which confer survival advantages and drug resistance. Defining the sequelae of myeloma cell interactions within these microenvironments on an individualized basis may provide the rational for personalized therapies; however, there are limited 3D models capable of mirroring patient plasma cell niches. To mimic the myeloma cell niche, here we describe a 3D *ex-vivo* model in which primary patient bone marrow cells are cultured in a collagen hydrogel matrix. In this 3D hydrogel model, prolonged survival of malignant plasma cells was observed after five days of culture.

3.2 Introduction

Multiple myeloma (MM) is the second most common hematological malignancy that is characterized by aggregation and proliferation of malignant plasma cells (PCs) within the bone marrow (BM). These cancerous PCs are

influenced by their tumor microniche in addition to genetic abnormalities.[85] Particularly, fibroblasts/stromal cells, endothelial cells, immune cells, and the extracellular matrix (ECM) have profound effects on MM cells. Collagen type I, collagen type IV, fibronectin, and laminin are critical ECM proteins present within the BM, with collagen type I and fibronectin predominating.[34,76] The interactions between myeloma cells and the supporting BM microenvironment plays critical roles in pathogenesis, mediating resistance to cell death, sustained proliferation, cell homing and invasion, and immunosuppression, thereby promoting MM progression.[86] Therefore, characterizing the efficacy of novel agents should not only assess the impact on myeloma cells, but also define effects on the tumor microenvironment.[87,88]

Several impediments remain in the study of human plasma cells. There is a lack of *in vitro* systems that are able to culture and maintain long-lived plasma cells. In traditional 2D or planar cultures, PC survival is relatively short, typically around three days. Previous studies have demonstrated that in order to maintain their phenotype in culture, PCs require components of the tumor microenvironment such as essential survival factors and/or BM stromal cells.[28,33] These reports have also indicated that interleukin 6 (IL-6) supports the generation of plasma cells *in vitro*.

In MM patients, IL-6 has been identified as a key factor in pathogenesis by inhibiting apoptosis in myeloma cells. IL-6 also interacts with several factors involved in the development and progression of MM, such as adhesion molecules,

tumor suppressor genes, and oncogenes.[35,36] Clinically, MM patients have elevated serum levels of IL-6, which are associated with poor prognosis.[37]

Numerous preclinical studies have demonstrated novel anti-MM agents, which have not translated to patient clinical benefits. One of the many challenges in treating myeloma is its genomic and phenotypic heterogeneity. This may be due to limitations in drug testing without the appropriate tumor environment and/or the lack of 3D BM architecture seen in patients. An emphasis on using 3D *in vitro* models, instead of conventional planar methods, to create an experimental system recapitulating the specialized characteristics of the MM BM has been demonstrated previously using: ECM molecules such as collagen and/or fibronectin; specialized scaffolds including gelatin sponges or silk; microfluidic tissues, as well as bioreactor-based cultures.[51,53,89–92]

Previously, we have utilized type I collagen for numerous *in vivo* and *in vitro* models in various fields including cardiovascular tissues, valve development, the foreign body response, and others.[93–99] Since collagen type I is abundant within the plasma cell niche of myeloma cells, it seems logical to use collagen as a scaffold when attempting to generate 3D models of the BM microenvironment. From prior research, it is apparent that additional comprehensive, patient-specific studies are needed to thoroughly mimic and investigate the malignant myeloma niche.

Here, we introduce an *in vitro* 3D model to mimic the myeloma niche composed of patient-derived BM and myeloma cells embedded in a hydrogel 3D system. This hydrogel model allows for the study of cellular and extracellular

components in the myeloma microenvironment including hematopoietic, immune, and tumor cells. In this study, we investigated the prolonged survival of PCs in a collagen hydrogel that is capable of recapitulating the complex microenvironment, in a patient-specific manner. Results from multiple analytical approaches indicated that PCs in this 3D hydrogel system maintained their pathological phenotype for at least five days of culture, thus suggesting that patient-derived BM aspirates can be used to model key features of long-lived plasma cell malignant progression within this *in vitro* model.

3.3 Material and Methods

Patient Aspirates and Cell Isolation

Primary BM cells from patients with premalignant condition or MM were studied including monoclonal gammopathy of undetermined significance (MGUS), low MM (15-20% PCs), and high MM (60-70% PCs). Approval for these studies was obtained from Greenville Health System Institutional Review Board (IRB # Pro00067642). All patient samples were collected after informed consent per GCP guidelines. After BM aspiration, fresh BM leukocytes were obtained by ammonium chloride based-lysis of red blood cells. Isolated BM cells were washed in 0.5% bovine serum albumin in phosphate-buffered saline (BSA/PBS) twice and then complete RMPI1640 media supplemented with 10% fetal bovine serum, 100U/mL penicillin, 100μg/mL streptomycin, and 250μg/mL amphotericin B.

Generation of 3D Constructs

Type I collagen (no. C857; Elastin Products Co. Owensville, MO USA) was diluted in 0.01M acetic acid to a concentration of 10mg/mL. Isolated patient cells (1.0×10^6 cells/mL) were gently incorporated into the collagen at a ratio of 1:2 (cell suspension: collagen) prior to 100 μL of the mixture being carefully added to a 96-well plate. The well plate was incubated for 20 min at 37°C in 5% CO_2 to allow for gelation and polymerization. After initial incubation, complete RMPI1640 media +/- IL-6 (10ng/mL) was added and changed two times over a period of 40 min to equilibrate the growth environment to physiological pH. Fresh media was added and constructs were gently dissociated from the walls of the well plates and cultured up to 5 days at 37°C in 5% CO_2.

Enzyme-Linked Immunosorbent Array (ELISA)

Isolated patient cells were seeded within type I collagen as previously described and supernatants were collected after one and five days of culture. Particulates were removed by centrifugation for 10 min at 1,500 rpm prior to being aliquoted and stored at -80°C until analysis. For analysis, supernatants were diluted at a ratio of 1:4 and the Human IgG ELISA (no. ab195215; Abcam Cambridge, MA USA) was used according to manufacturer's instructions.

Immunofluorescence

The three-dimensional collagen constructs were collected after one and five days of culture and placed into 4% paraformaldehyde. The constructs were

permeabilized with 0.1% Triton X-100/PBS three times for 15 min each followed by a 0.3M Glycine wash for 30 min. Collagen gels were rinsed with PBS and blocked in 2% BSA/PBS for 1 hour at room temperature. Samples were incubated in primary antibodies [1:100] in 1%BSA/PBS overnight at 4°C. Collagen gels were stained with CD138 (no.PA5-16918; Thermo Fisher, Waltham, MA USA). Then, constructs were rinsed with 1%BSA/PBS two times for 15 min each and 1X PBS for 15 min prior to incubating with appropriate secondary antibodies [1:100] in 1%BSA/PBS for 1 hour at 37°C (Alexa 488 no. A11034; Thermo Fisher, Waltham, MA USA). Collagen gels were rinsed three times in PBS for 15 min each prior to being counterstained with DAPI [1:5000] for 20 min at room temperature. After a final rinse in PBS, constructs were mounted with deionized water and imaged at 25X on the Lecia SP8 multiphoton confocal microscope.

The percentage of plasma cells per patient construct was quantified by dividing the number CD138+ cells by the total number of nuclei. Four random fields were imaged per constructs and the average percentage was calculated.

Statistical Analysis

Statistical analysis to evaluate changes in IgG levels and in the percentage of CD138+ cells were determined by 2-way analysis of variance and Sidak's multiple comparisons test. Data are reported as mean ± SD. Differences between groups were considered significant at $P < 0.05$.

3.4 Results

To mimic the neoplastic BM microniche of myeloma cells, patient BM leukocytes were cultured in a hydrogel-based 3D model. In the 3D model, PCs at premalignant and malignant stages of MM remained viable five days after culture (Figure 3.1).

Characterization of Patient Constructs

Monoclonal Gammopathy of Undetermined Significance

Bone marrow aspirates were collected and processed for patients undergoing screening for premalignant MGUS. To verify the viability of MGUS leukocytes within the collagen constructs, supernatants were analyzed for changes in IgG concentration after five days of culture. Overall, MGUS 3D collagen constructs exhibited a lower concentration of IgG production by day 5 despite the addition of IL-6. There was an increase in IgG concentration from day 1 to day 5 when patient #1030 and #1032 constructs were cultured without IL-6 (Figure 3.2). A significant decrease in IgG was observed by day 5 when patient 1030 collagen gels were cultured in the presence of IL-6. Additionally, there was a decrease in IgG concentration for patient #1032 when cultured with IL-6, though this difference was not significant (Figure 3.2). Collagen constructs then were stained with CD138, a plasma cell marker, to determine changes in the percentage of PCs within the gels over five days. There was an increase in CD138+ cells within patient #1030 and #1032 constructs by day five, regardless of treatment with IL-6 (Figure 3.1 A, B, Figure 3.3)

Multiple Myeloma, 15-20% Plasma Cells

Isolated leukocytes from MMpatients that present with 15-20% monoclonal plasma cells were embedded within the collagen hydrogel. Patient #1027 showed significant increases in IgG concentration between day 1 and day 5 when cultured with or without IL-6 (Figure 3.4). Additionally, there was an increase in the percentage of CD138+ cells by day 5 when constructs were cultured with or without IL-6, though this difference was not significant (Figure 3.5, Figure 3.1 C, D). Patient #1033 exhibited a significant increase in IgG concentration between day 1 and day 5 when cultured without IL-6. When constructs were cultured in the presence of IL-6, IgG concentration in patient #1033 constructs remained constant over five days (Figure 3.4). Increases in the percentage of CD138+ PCs were seen from day 1 to day 5 when constructs were cultured with or without IL-6, though these increases were not significant (Figure 3.5).

Multiple Myeloma, 60-70% Plasma Cells

Isolated cells from myeloma patients with 60-70% plasma cells were also cultured within the collagen gel. There was a significant decrease seen in IgG concentration for patient #1022 and #1034 constructs by day 5 when cultured without IL-6; however, when cultured in the present of IL-6, there was a significant increase in IgG by day 5 for both patients (Figure 3.6). There were decreases in the percentage of CD138+ PCs from day 1 to day 5 when constructs were cultured without IL-6 for both patients (Figure 3.7). When cultured with IL-6, there was a significant increase in CD138+ cells for patient #1022 from day 1 to day 5.

Additionally, patient #1034 constructs also exhibited an increase in CD138+ cells when cultured with IL-6, though this increase was not significant (Figure 3.7, Figure 3.1 E, F).

3.5 Discussion

Multiple myeloma remains an incurable disease due to challenges in treatment due to genomic and phenotypic heterogeneity.[6,16] This may also be due to limitations in therapeutic testing without the supporting tumor microenvironment and/or the lack of BM architecture that is seen within patients. Numerous 2D, planar models have demonstrated novel MM agents that have not translated to *in vivo* benefits. Research has shown that the tumor microniche is critical for the maintenance and progression for myeloma cells. This study utilized type I collagen to create 3D patient specific constructs. Results indicate that isolated BM leukocytes from premalignant and malignant myeloma patients maintained their pathological phenotype for at least five days of culture within the collagen, which is well beyond typical short-lived plasma cell cultures. While future studies involving further manipulation and analysis is required, this 3D hydrogel-based model presented provides an innovative method for gaining insight in MM disease progression from premalignant MGUS to active MM.

In this study, the expression level of IgG was utilized as a functional assay to determine plasma cell viability after five days of culture. Furthermore, constructs were stained and imaged to determine the percentage of CD138+ plasma cells during the culture period. First, patient constructs cultured without IL-6 were

analyzed. Expression levels of IgG increased after five days in MGUS constructs despite patient to patient variation. An increase was also seen in the percentage of CD138+ cells within the MGUS gels. These results suggest that we have maintained the pathological PC phenotype of MGUS patients for at least five days of culture. MM constructs containing 15-20% PCs displayed a significant increase in IgG concentration. Furthermore, this increase was also seen in the percentage of CD138+ cells, though not significant. Further supporting that long-lived plasma cells can be maintained within this 3D collagen model, as components of their specific tumor microenvironment provided the critical essential factors necessary for their survival. Interestingly, in myeloma constructs with 60-70% PCs there was a significant decrease in IgG production and decreases in the percentage of plasma cells. These results suggest there was potentially a limited number of necessary supporting microenvironment factors within the collagen cultures, which is expected due to the high percentage of monoclonal cells in the BM cellularity. These high myeloma constructs indicated the importance of the *in vivo* tumor microniche for the *in vitro* study of long-lived plasma cells because without these essential components or additional factors introduced, plasma cells are unable to survive for five days *in vitro*. [21,28,33]

Interleukin-6 is a key essential survival factor in MM that has been shown to play critical roles in maintaining the growth and expansion of plasma cells within the BM.[33,35,36,100–102] IL-6 is key in MM progression and pathogenesis by inhibiting PC apoptosis, while interacting with other factors involved in the development of MM. Additionally, IL-6 plays a key role in supporting the maintenance of long-lived

plasma cells *in vitro*.[23,103,104] In this study, IL-6 played an important role in maintaining the long-lived plasma cells. When MGUS constructs were cultured in the presence of IL-6, paradoxically there was a decrease in IgG concentration, but there was an increase in the percentage of plasma cells within the constructs after five days of culture. Though IgG concentration decreased by day 5 in MGUS constructs, the increase of CD138+ cells suggests that IL-6 can support myeloma cell maintenance in cultures. Since these MGUS patients presented with lower serum IgG levels compared to the myeloma patients, perhaps IgG was not an appropriate validation assay for these patients as MGUS and myeloma patients can also produce high levels of IgA or light chain only immunoglobulins.[105,106]

In comparison to MGUS constructs, MM constructs, 15-20% and 60-70%, exhibited significant increases in IgG concentration after five days of culture. Additionally, there were increases in the percentage of CD138+ cells within the patient constructs after five days. Overall, findings in the myeloma constructs supports previous studies which demonstrated that IL-6 is an important factor in culturing long-lived plasma cells.[107–109]

The patient derived 3D collagen model described in the study is capable of maintaining myeloma cell viability for at least five days of culture. This creates a critical experimental window in which PC/MM cell biology can be explored. The broader applications of this work include detailed analysis of the long-lived plasma cell survival microniche as it transitions from its primary role in humoral function to a pathogenic role as in MM. Furthermore, results from this project will lead to the development of high-fidelity human models of normal and pathological myeloma

BMs. Though this preliminary study needs to be further validated in prospective trials, the results do suggest that our 3D culture system may be utilized to predict the clinical utility of novel myeloma therapies.

3.6 Conclusions

In this study, an *in vitro* 3D model to mimic the myeloma cell niche was introduced using patient derived BM and myeloma cells which were embedded in a 3D hydrogel-based system. Importantly, the 3D patient cultures maintained the pathological phenotype of plasma cells for at least five days of culture. Therefore, providing a patient specific model to explore the growth of MM clones associated with therapeutic resistance and the transition of long-lived PCs from humoral function to malignancy. Ultimately, the 3D collagen constructs may asses tumor sensitivity to conventional and novel anti-MM therapies, and thereby inform single agent or combination individualized therapy.

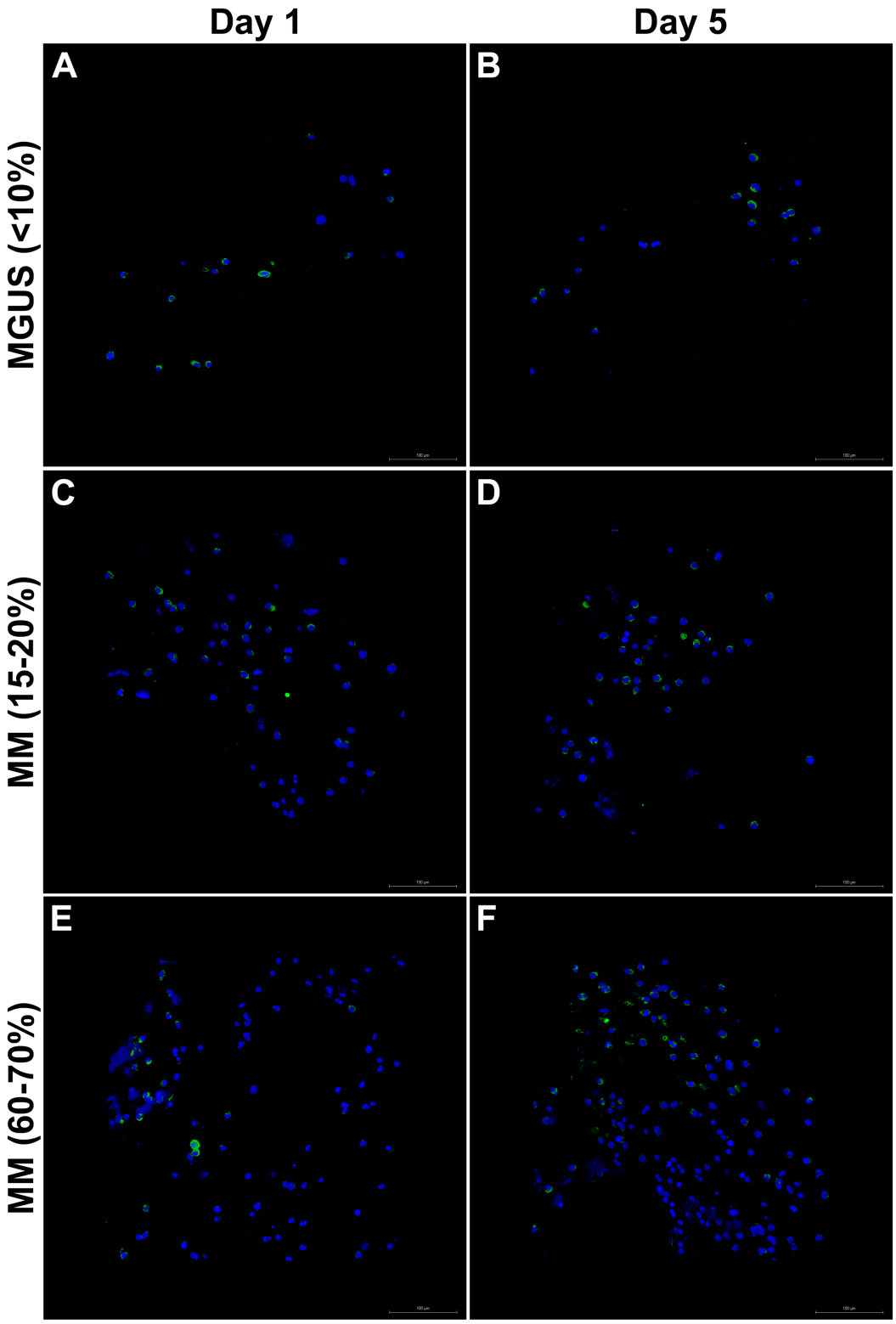

Figure 3.1. Isolated patient BM leukocytes were cultured in a 3D collagen-based model of multiple myeloma. Blue shows nuclei and green shows CD138, a plasma cell marker. Scale Bar: 100μm.

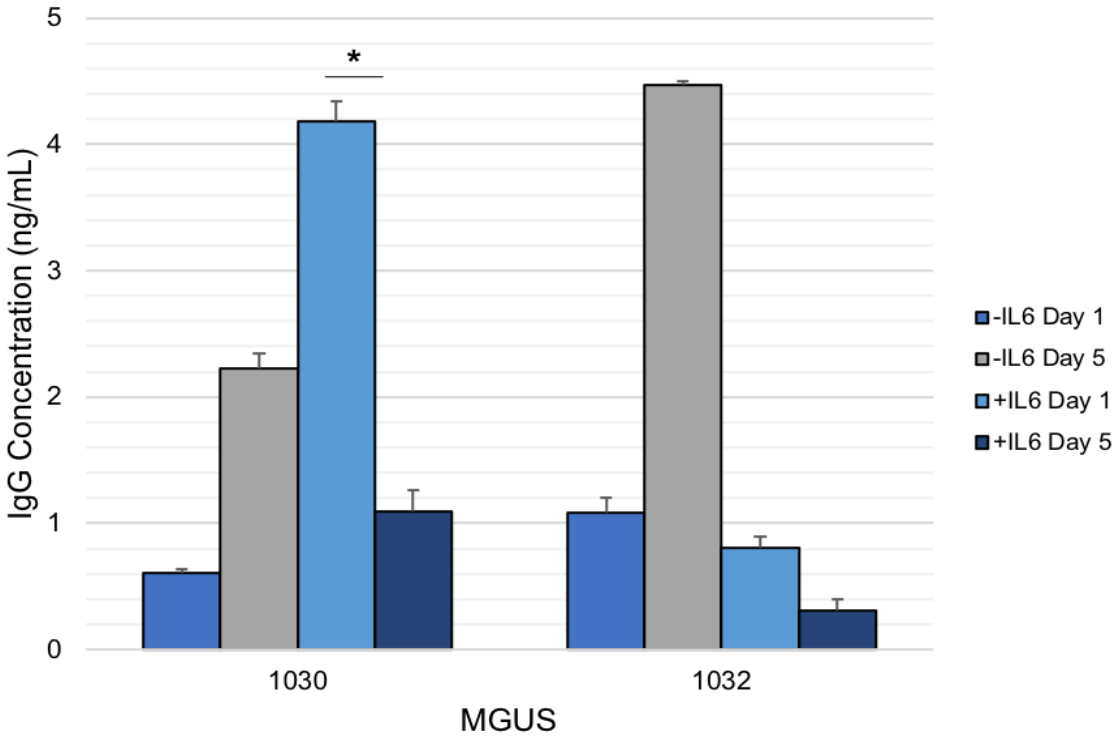

Figure 3.2. IgG concentration in MGUS collagen constructs. MGUS patients exhibit an increase in IgG expression levels five days after culture, however the addition of IL-6 decreased IgG concentration in patient gels. * $P < 0.05$.

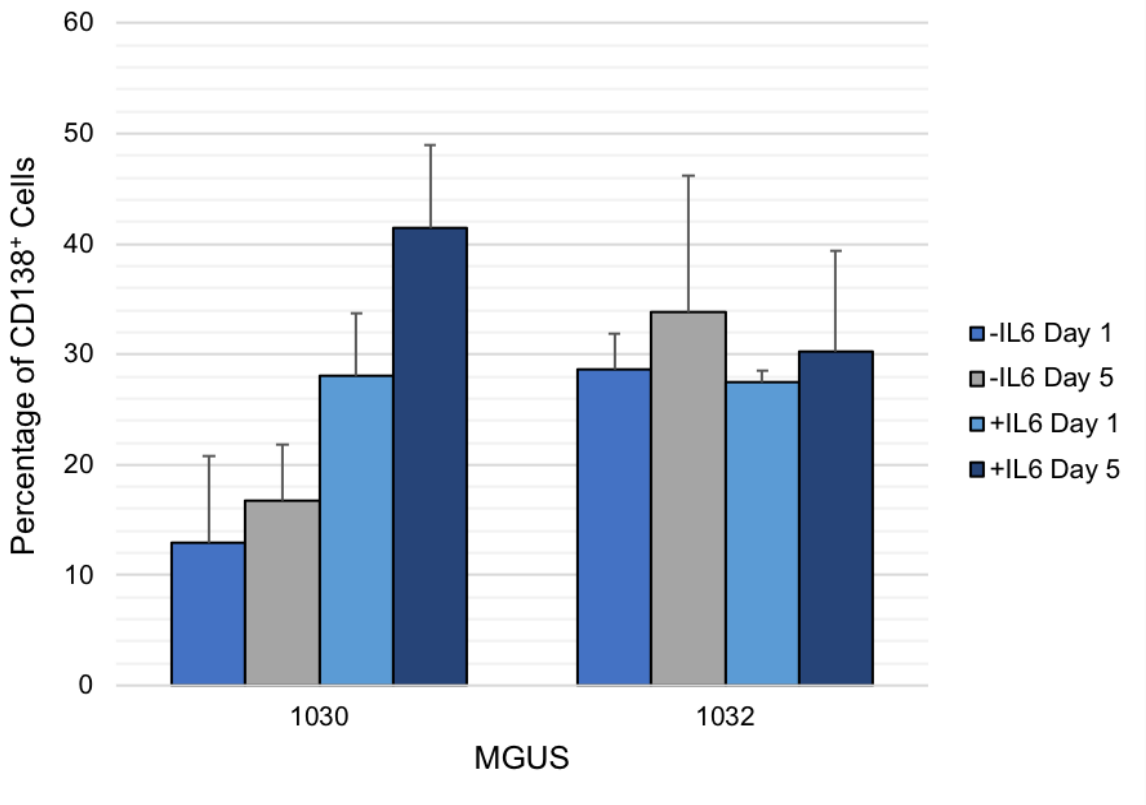

Figure 3.3.The percentage of CD138+ plasma cells increased from day 1 to day 5 when isolated MGUS patient cells were cultured in the collagen gel, with or without IL-6.

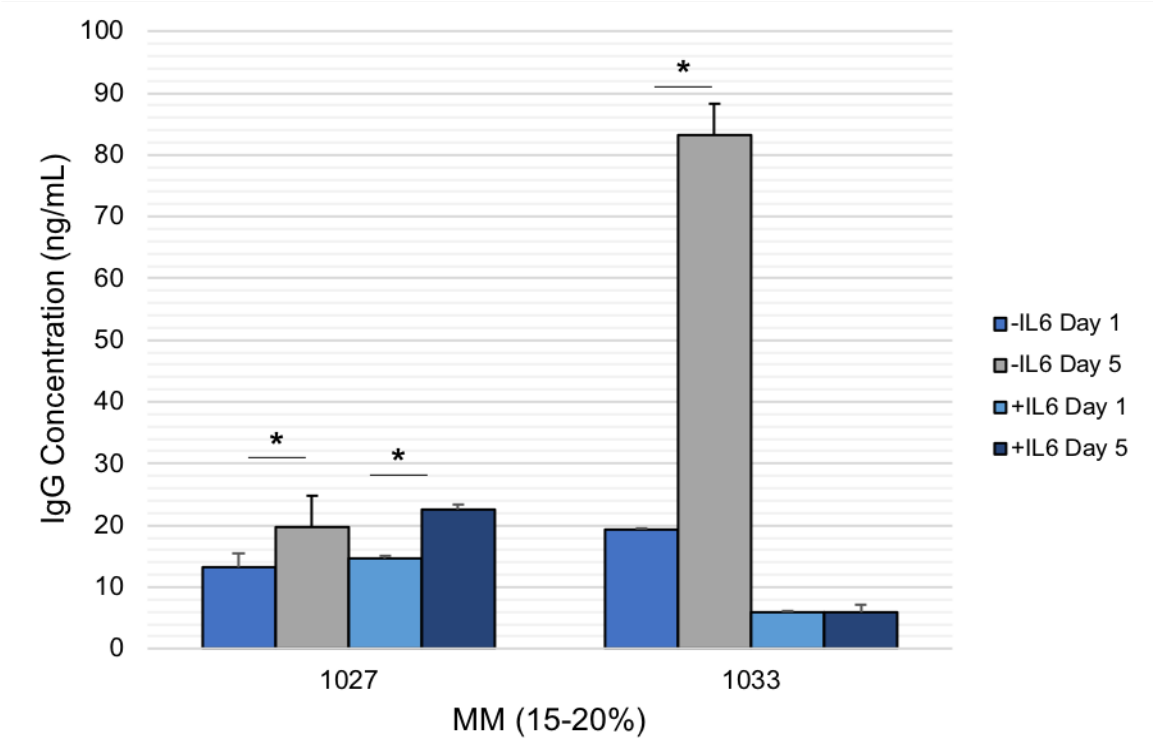

Figure 3.4. MM patient (15-20% plasma cells) cell constructs cultured without IL-6 demonstrated a significant increase in IgG expression levels after five days of culture. The addition of IL-6 to the gels resulted in a significant increase in IgG concentration for patient #1027, while patient #1033's levels remained constant during the culture period. * $P < 0.05$

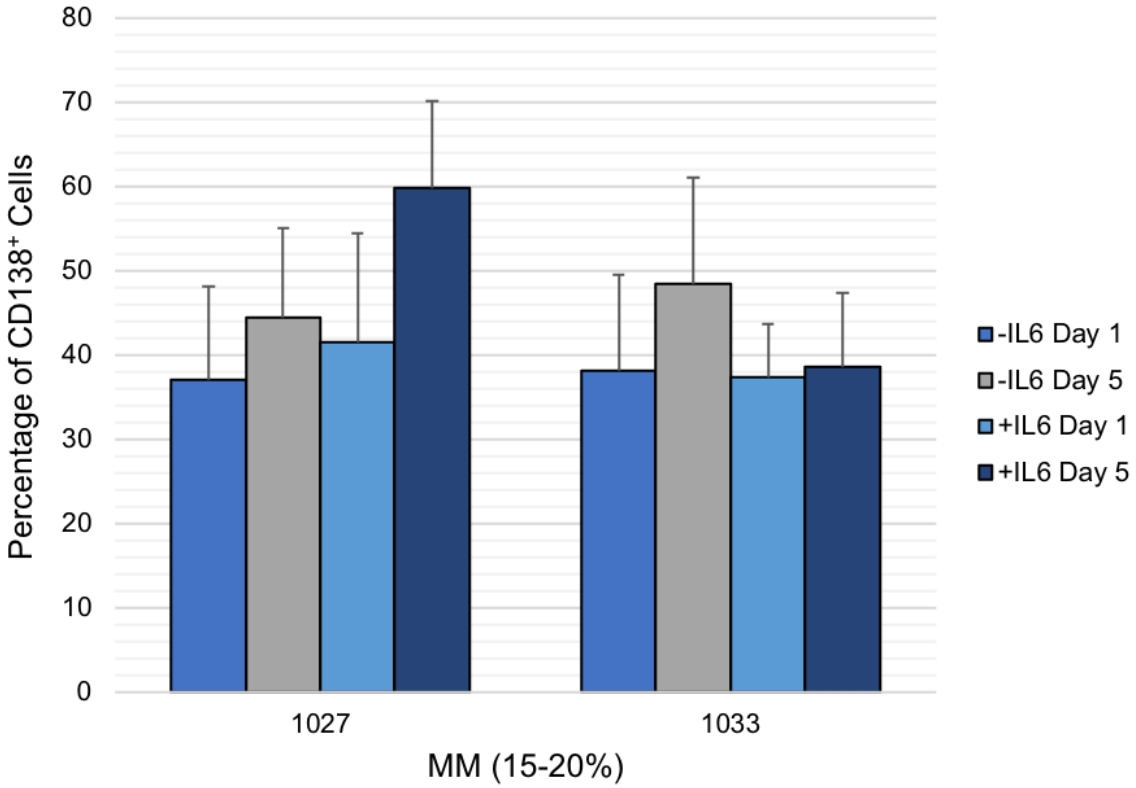

Figure 3.5. BM cells isolated from multiple myeloma patients with 15-20% monoclonal plasma cells exhibited an overall increase in CD138+ cells from day 1 to day 5, with or without the addition of IL-6.

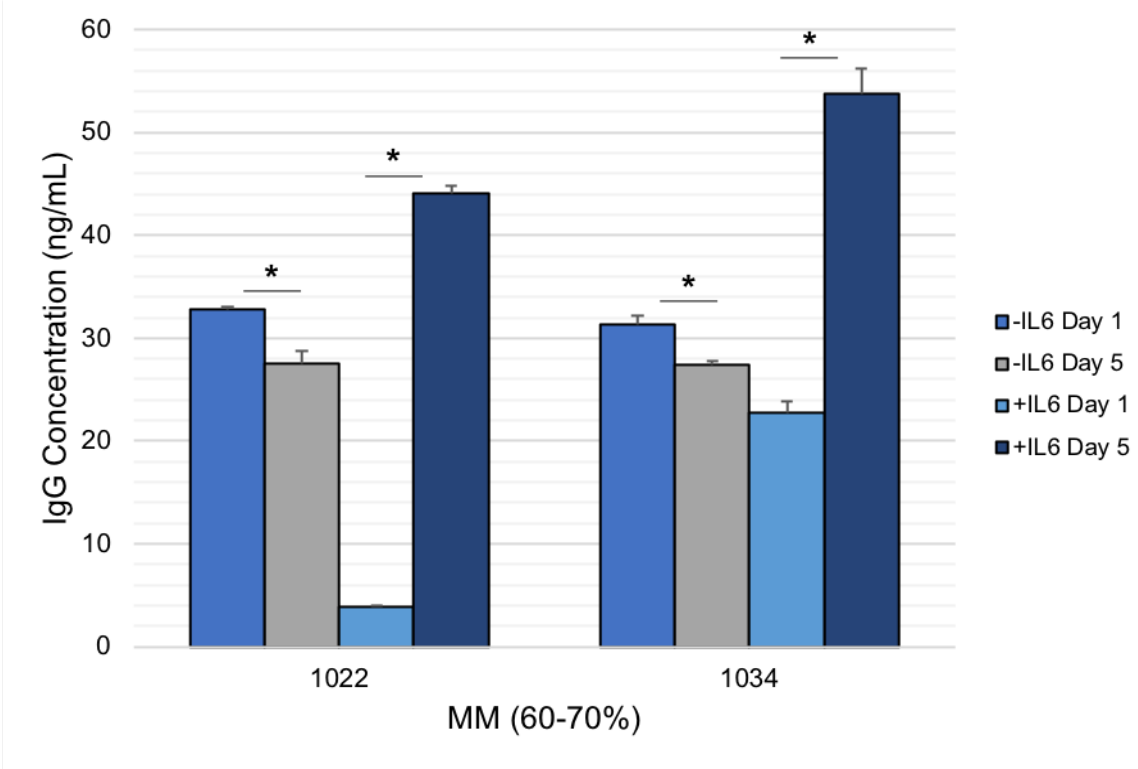

Figure 3.6. MM (60-70% clonal plasma cells) constructs demonstrate significant decreases in IgG concentration when not cultured in the presence of IL-6. Culturing the constructs with IL-6 resulted in a significant increase in IgG expression from day 1 to day 5. * $P < 0.05$.

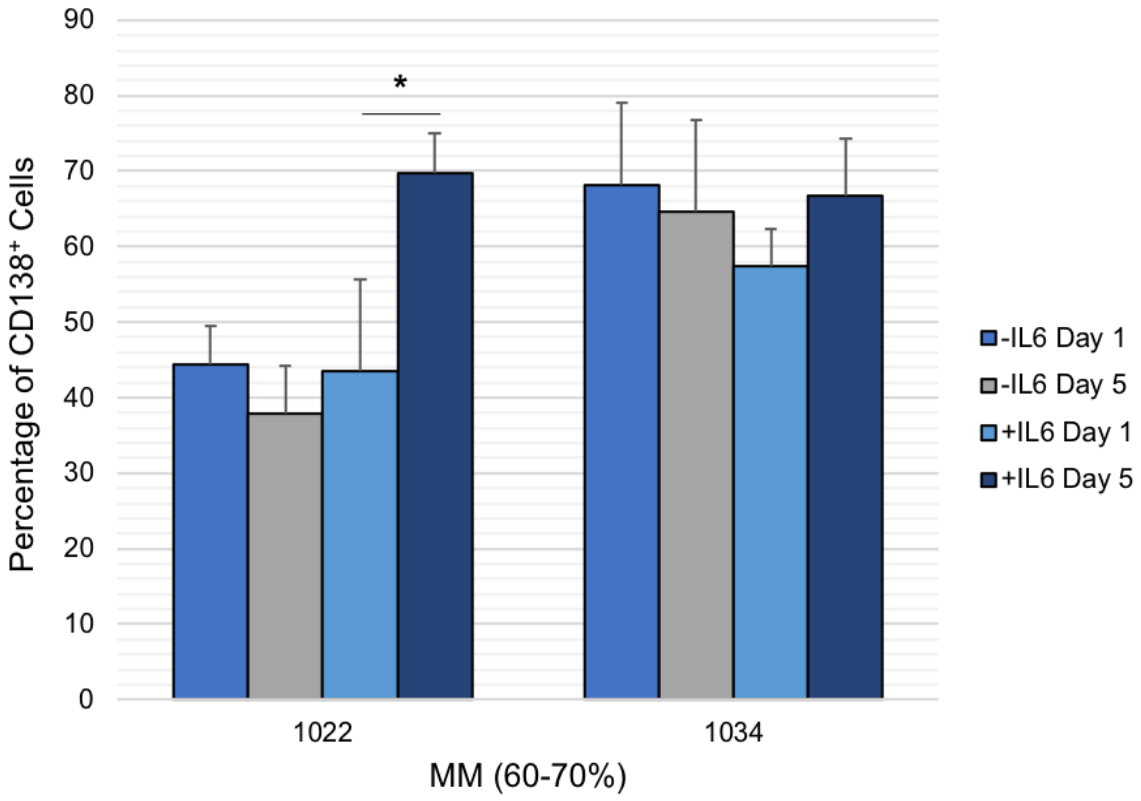

Figure 3.7.MM (60-70% clonal plasma cells) constructs demonstrate decreases in the percentage of CD138+ cells when not cultured in the presence of IL-6. With the addition of IL-6 to the culture, the percentage of plasma cells increased by day 5. * $P < 0.5$.

CHAPTER 4

CONCLUSIONS

4.1 Summary

Multiple myeloma (MM) remains an incurable disease due to the high clonal heterogeneity of myeloma cells and its clinical repercussions. Furthermore, heterogeneity is found in regard to disease onset, disease progression, therapeutic resistance, and subsequent patient relapse. This project investigated differences in the BM microenvironment of MGUS and MM cells, while also generating a patient specific collagen-based three-dimensional *in vitro* model of the disease which allows for investigation of the complex interactions in the plasma cell niche.

Results from this study have demonstrated that increases in extracellular matrix, specifically fibronectin expression, are related to disease transition from MGUS to MM. Furthermore, morphological changes in plasma cells were also exhibited. Electron micrographs displayed increases in ER and densely packed vesicles associated with myeloma patients, which was not seen in premalignant patients. Additionally, autophagosomes were present in both MGUS and MM patients, as denoted by LC3 staining. These results demonstrate the need to further define the three-dimensional BM microenvironment and plasma cell niche

as it can provide further insight into therapeutic treatments of this incurable disease.

This project also introduced a patient-specific 3D *in vitro* model capable of mimicking the myeloma cell niche by embedding BM derived cells in a hydrogel-based system. This 3D model was capable of maintaining the pathological phenotype of plasma cells for at least five days of culture. By providing a patient specific model, this study will help to explore the growth of MM clones associated with therapeutic resistance and the transition of long-lived PCs from humoral function to malignancy. These constructs could asses tumor sensitivity to conventional and novel anti-MM therapies, and thereby inform single agent or combination individualized therapy. Validation of this model will provide a test bed for other long-lived PC applications such as using these cells for the production of human monoclonal antibodies *in vitro*. Moreover, if successful, the results of this project will lead to the development of high-fidelity human models of normal and pathological BMs.

4.2 Future Directions

While this study has identified expression changes of fibronectin, the investigation of other ECM proteins such as collagen I, collagen IV, and laminin would provide even greater insight into the BM microenvironment as it relates to disease progression. Three-dimensional mapping of the malignant BM and plasma cell niche can provide critical information to the spatial distribution and the localization and colocalization of key myeloma markers, which can provide novel

targets for the treatment of MM. Additionally, autophagy is important in MM disease progression. As normal and malignant PCs varies within each patient, identification of which phenotype of plasma cells presents with autophagosomes could provide valuable insight.

An emphasis on utilizing 3D *in vitro* models, instead of conventional 2D planar methods, to create an experimental system recapitulating the specialized characteristics of the MM BM has been previously demonstrated. However, additional models of comprehensive patient specific studies are needed to thoroughly mimic and investigate the malignant myeloma niche. Though we have created a patient-specific model of MM, further validation of this model is needed to determine the difference between plasma cell survival and proliferation, as normal long-lived PCs exhibit survival with minimal proliferation. Furthermore, qPCR experiments examining essential survival factors between MGUS and MM patient constructs will help to define the 3D patient models. The ultimate goal for these 3D constructs is to create a high-fidelity test bed for current and novel MM therapeutic agents. Using this culture system, therapeutics can be tested in patient-specific manner. This potential bench to beside approach could help clinicians to determine if single or combination treatments may be best for their patients, increasing the survival rate of MM patients and potentially curing the disease.

REFERENCES

1. Siegel RL, Miller KD, Jemal A. Cancer statistics, 2019. *CA Cancer J Clin*. 2019;69(1):7-34. doi:10.3322/caac.21551.
2. Siegel RL, Miller KD, Jemal A. Cancer Statistics, 2017. *CA Cancer J Clin*. 2017;67(1):7-30. doi:10.3322/caac.21387.
3. Di Marzo L, Desantis V, Solimando AG, et al. Microenvironment drug resistance in multiple myeloma: emerging new players. *Oncotarget*. 2016;7(37):60698-60711. doi:10.18632/oncotarget.10849.
4. Oracki SA, Walker JA, Hibbs ML, Corcoran LM, Tarlinton DM, Tarlinton DM. Plasma cell development and survival. *Immunol Rev*. 2013;237:140-159.
5. Wickramasinghe SN, Porwit A, Erber WN. *Normal Bone Marrow Cells. Development and Cytology.* Second Edi. Elsevier Ltd; 2011. doi:10.1016/B978-0-7020-3147-2.00002-X.
6. Kumar S, Kimlinger T, Morice W. Immunophenotyping in multiple myeloma and related plasma cell disorders. *Best Pract Res Clin Haematol*. 2010;23(3):433-451. doi:10.1016/j.beha.2010.09.002.
7. Fairfax KA, Kallies A, Nutt SL, Tarlinton DM. Plasma cell development: From B-cell subsets to long-term survival niches. *Semin Immunol*. 2008;20(1):49-58. doi:10.1016/j.smim.2007.12.002.
8. Nutt SL, Fairfax KA, Kallies A. BLIMP1 guides the fate of effector B and T cells. *Nat Rev Immunol*. 2007;7(12):923-927. doi:10.1038/nri2204.

9. Fairfield H, Falank C, Avery L, Reagan MR. Multiple myeloma in the marrow: pathogenesis and treatments. *Ann N Y Acad Sci*. 2016;1364(1):32-51. doi:10.1111/nyas.13038.

10. Zimmerman T. *Plasma Cell Dyscrasias*. Vol 169. (Roccaro AM, Ghobrial IM, eds.). Cham: Springer International Publishing; 2016. doi:10.1007/978-3-319-40320-5.

11. Rajkumar SV, Kumar S. Multiple Myeloma: Diagnosis and Treatment. *Mayo Clin Proc*. 2016;91(1):101-119. doi:10.1016/j.mayocp.2015.11.007.

12. Kawano Y, Moschetta M, Manier S, et al. Targeting the bone marrow microenvironment in multiple myeloma. *Immunol Rev*. 2014;263:160-172.

13. Manier S, Sacco A, Leleu X, Ghobrial IM, Roccaro AM. Bone marrow microenvironment in multiple myeloma progression. *J Biomed Biotechnol*. 2012;2012. doi:10.1155/2012/157496.

14. Fairfield H, Falank C, Avery L, Reagan MR. Multiple myeloma in the marrow: Pathogenesis and treatments. *Ann N Y Acad Sci*. 2016;1364(1):32-51. doi:10.1111/nyas.13038.

15. Palumbo A, Anderson K. Multiple Myeloma. *N Engl J Med*. 2011;364(11):1046-1060. doi:10.1056/NEJMra1011442.

16. Kuehl WM, Bergsagel PL. Molecular pathogenesis of multiple myeloma and its premalignant precursor. *J Clin Invest*. 2012;122(10):3456-3463. doi:10.1172/JCI61188.

17. Glavey S V., Leung N. Monoclonal gammopathy: The good, the bad and the ugly. *Blood Rev*. 2016;30(3):223-231. doi:10.1016/j.blre.2015.12.001.

18. Bergsagel PL, Kuehl WM. Molecular pathogenesis and a consequent classification of multiple myeloma. *J Clin Oncol*. 2005;23(26):6333-6338. doi:10.1200/JCO.2005.05.021.

19. Weiss BM, Abadie J, Verma P, Howard RS, Kuehl WM. A monoclonal gammopathy precedes multiple myeloma in most patients. *Blood*. 2009;113(22):5418-5422. doi:10.1182/blood-2008-12-195008.

20. Kyle RA, Therneau TM, Rajkumar SV, et al. A Long-Term Study of Prognosis in Monoclonal Gammopathy of Undetermined Significance. *N Engl J Med*. 2002;346(8):564-569. doi:10.1056/NEJMoa01133202.

21. Schwendener RA, Mete S. A New Approach to Cancer Therapy: The Tumor Microenivornment as Target. *Front Clin Drug Res Anti-Cancer Agents*. 2014;1:3-68.

22. Guillerey C, Nakamura K, Vuckovic S, Hill GR, Smyth MJ. Immune responses in multiple myeloma: Role of the natural immune surveillance and potential of immunotherapies. *Cell Mol Life Sci*. 2016;73(8):1569-1589. doi:10.1007/s00018-016-2135-z.

23. Lauta VM. A review of the cytokine network in multiple myeloma: Diagnostic, prognostic, and therapeutic implications. *Cancer*. 2003;97(10):2440-2452. doi:10.1002/cncr.11072.

24. Garcia-Gomez A. Multiple myeloma mesenchymal stromal cells: Contribution to myeloma bone disease and therapeutics. *World J Stem Cells*. 2014;6(3):322. doi:10.4252/wjsc.v6.i3.322.

25. Hideshima T, Mitsiades C, Tonon G, Richardson PG, Anderson KC. Understanding multiple myeloma pathogenesis in the bone marrow to identify new therapeutic targets. *Nat Rev Cancer*. 2007;7(8):585-598. doi:10.1038/nrc2189.

26. Vincent T, Mechti N. Extracellular matrix in bone marrow can mediate drug resistance in myeloma. *Leuk Lymphoma*. 2005;46(6):803-811. doi:10.1080/10428190500051448.

27. Fei M, Hang Q, Hou S, Ruan C. Cell adhesion to fibronectin down-regulates the expression of Spy1 and contributes to drug resistance in multiple myeloma cells. *Int J Hematol*. 2013;98(4):446-455. doi:10.1007/s12185-013-1435-4.

28. Cassese G, Arce S, Hauser AE, et al. Plasma Cell Survival Is Mediated by Synergistic Effects of Cytokines and Adhesion-Dependent Signals. *J Immunol*. 2003;171(4):1684-1690. doi:10.4049/jimmunol.171.4.1684.

29. Wols HAM, Underhill GH, Kansas GS, Witte PL. The Role of Bone Marrow-Derived Stromal Cells in the Maintenance of Plasma Cell Longevity. *J Immunol*. 2014;169(8):4213-4221. doi:10.4049/jimmunol.169.8.4213.

30. Wardemann H, Ellyard MCN, I J, et al. Antigen-selected, immunoglobulin-secreting cells persist in human spleen and bone marrow. *Blood*. 2004;103(10):3805-3812. doi:10.1182/blood-2003-09-3109.Supported.

31. Mahindra A, Laubach J, Raje N, Munshi N, Richardson PG, Anderson K. Latest advances and current challenges in the treatment of multiple myeloma. *Nat Rev Clin Oncol*. 2012;9:135-143.

32. Chatterjee M, Ho D, Lentzsch S, et al. In the presence of bone marrow stromal cells human multiple myeloma cells become independent of the IL-6 / gp130 / STAT3 pathway. *Cell*. 2002;100(9):3311-3318. doi:10.1182/blood-2002-01-0102.Supported.

33. Cretu A, Brooks PC. Impact of the Non-Cellular Tumor Microenvironment on Metastasis: Potential Therapeutic and Imaging Opportunities. *J Cell Physiol*. 2007;213:391-402. doi:10.1002/JCP.

34. Tancred TM, Belch AR, Reiman T, Pilarski LM, Kirshner J. Altered Expression of Fibronectin and Collagens I and IV in Multiple Myeloma and Monoclonal Gammopathy of Undetermined Significance The Journal of Histochemistry & Cytochemistry. *Histochemistry*. 2009;57(3):239-247. doi:10.1369/jhc.2008.952200.

35. Scheller J, Chalaris A, Schmidt-Arras D, Rose-John S. The pro- and anti-inflammatory properties of the cytokine interleukin-6. *Biochim Biophys Acta - Mol Cell Res*. 2011;1813(5):878-888. doi:10.1016/j.bbamcr.2011.01.034.

36. Yao X, Huang J, Zhong H, et al. Targeting interleukin-6 in inflammatory autoimmune diseases and cancers. *Pharmacol Ther*. 2014;141(2):125-129. doi:10.1016/j.pharmthera.2013.09.004.

37. Taniguchi K, Karin M. IL-6 and related cytokines as the critical lynchpins between inflammation and cancer. *Semin Immunol*. 2014;26(1):54-74. doi:10.1016/j.smim.2014.01.001.

38. Novak AJ, Darce JR, Arendt BK, et al. Expression of BCMA, TACI, and BAFF-R in multiple myeloma: A mechanism for growth and survival. *Blood*. 2004;103(2):689-694. doi:10.1182/blood-2003-06-2043.

39. O'Connor BP, Raman VS, Erickson LD, et al. BCMA is essential for the survival of long-lived bone marrow plasma cells. *J Exp Med*. 2004;199(1):91-98. doi:10.1084/jem.20031330.

40. Tai YT, Acharya C, An G, et al. APRIL and BCMA promote human multiple myeloma growth and immunosuppression in the bone marrow microenvironment. *Blood*. 2016;127(25):3225-3236. doi:10.1182/blood-2016-01-691162.

41. Pan J, Sun Y, Zhang N, et al. Characteristics of BAFF and APRIL factor expression in multiple myeloma and clinical significance. *Oncol Lett*. 2017;14(3):2657-2662. doi:10.3892/ol.2017.6528.

42. Wang M, Wu D, Liu P, Deng J. Silence of MCL-1 upstream signaling by shRNA abrogates multiple myeloma growth. *Exp Hematol Oncol*. 2014;3(1):27. doi:10.1186/2162-3619-3-27.

43. Wuillème-Toumi S, Robillard N, Gomez P, et al. Mcl-1 is overexpressed in multiple myeloma and associated with relapse and shorter survival. *Leukemia*. 2005;19(7):1248-1252. doi:10.1038/sj.leu.2403784.

44. Quinn BA, Dash R, Azab B. Targeting Mcl-1 for the therapy of cancer. *Expert Opin Investig Drugs*. 2011;20(10):1397-1411. doi:10.1517/13543784.2011.609167.

45. Peperzak V, Vikstrom I, Walker J, et al. Mcl-1 is essential for the survival of plasma cells. *Nat Immunol*. 2013;14(3):290-297. http://dx.doi.org/10.1038/ni.2527.

46. Quach H, Ritchie D, Stewart AK, et al. Mechanism of action of immunomodulatory drugs (IMiDS) in multiple myeloma. *Leukemia*. 2010;24(1):22-32. doi:10.1038/leu.2009.236.

47. Piperdi B, Ling Y-H, Liebes L, Muggia F, Perez-Soler R. Bortezomib: Understanding the Mechanism of Action. *Mol Cancer Ther*. 2011;10(11):2029-2030. doi:10.1158/1535-7163.MCT-11-0745.

48. Yang W-C, Lin S-F. Mechanisms of Drug Resistance in Relapse and Refractory Multiple Myeloma. *Biomed Res Int*. 2015;2015:1-17. doi:10.1155/2015/341430.

49. Mateos MV, San Miguel JF. How should we treat newly diagnosed multiple myeloma patients? *Hematology Am Soc Hematol Educ Program*. 2013;2013:488-495. doi:10.1182/asheducation-2013.1.488.

50. Jurczyszyn A, Zebzda A, Czepiel J, et al. The Analysis of the Relationship between Multiple Myeloma Cells and Their Microenvironment. *J Cancer*. 2015;6(2):160-168. doi:10.7150/jca.10873.

51. Kirshner J, Thulien KJ, Martin LD, et al. A unique three-dimensional model for evaluating the impact of therapy on multiple myeloma. *Blood*. 2008;112(7):2935-2946. doi:10.1182/blood-2008-02-142430.An.

52. Sharma MB, Limaye LS, Kale VP. Mimicking the functional hematopoietic stem cell niche in vitro: Recapitulation of marrow physiology by hydrogel-based three-dimensional cultures of mesenchymal stromal cells. *Haematologica*. 2012;97(5):651-660. doi:10.3324/haematol.2011.050500.

53. Jakubikova J, Cholujova D, Hideshima T, et al. A novel 3D mesenchymal stem cell model of the multiple myeloma bone marrow niche: biologic and clinical applications. *Oncotarget*. 2016;7(47). doi:10.18632/oncotarget.12643.

54. Reagan MR, Mishima Y, Glavey S V, et al. Novel 3D bone marrow niche model Investigating osteogenic differentiation in multiple myeloma using a novel 3D bone marrow niche model. *Blood*. 2014;124(22):3250-3259. doi:10.1182/blood-2014-02-558007.

55. Braham MVJ, Minnema MC, Aarts T, et al. Cellular immunotherapy on primary multiple myeloma expanded in a 3D bone marrow niche model. *Oncoimmunology*. 2018;0(0):1-13. doi:10.1080/2162402X.2018.1434465.

56. Munshi NC, Anderson KC. New Strategies in the Treatment of Multiple Myeloma. *Clin Cancer Res*. 2013;19(13):3337-3344. doi:10.1158/1078-0432.CCR-12-1881.

57. Gooding S, Edwards CM. New approaches to targeting the bone marrow microenvironment in multiple myeloma. *Curr Opin Pharmacol*. 2016;28:43-49. doi:10.1016/j.coph.2016.02.013.

58. Hideshima T, Bergsagel PL, Kuehl WM, Anderson KC. Advances in biology of multiple myeloma: clinical applications. *Blood*. 2004;104(3):607-618. doi:10.1182/blood-2004-01-0037.

59. Vincenz L, Jager R, O'Dwyer M, Samali A. Endoplasmic Reticulum Stress and the Unfolded Protein Response: Targeting the Achilles Heel of Multiple Myeloma. *Mol Cancer Ther*. 2013;12(6):831-843. doi:10.1158/1535-7163.mct-12-0782.

60. Nikesitch N, Lee JM, Ling S, Roberts TL. Endoplasmic reticulum stress in the development of multiple myeloma and drug resistance. *Clin Transl Immunol*. 2018;7(1):1-13. doi:10.1002/cti2.1007.

61. Prasad R, Yadav RR, Singh A, Mathur SP, Mangal Y, Singh M. Non-secretory multiple myeloma presenting with diffuse sclerosis of affected bones interspersed with osteolytic lesions. *Br J Radiol*. 2009;82(974). doi:10.1259/bjr/68683396.

62. Shen K, Johnson DW, Vesey DA, McGuckin MA, Gobe GC. Role of the unfolded protein response in determining the fate of tumor cells and the promise of multi-targeted therapies. *Cell Stress Chaperones*. 2018;23(3):317-334. doi:10.1007/s12192-017-0844-3.

63. Pengo N, Scolari M, Oliva L, et al. Plasma cells require autophagy for sustainable immunoglobulin production. *Nat Immunol*. 2013;14:298. https://doi.org/10.1038/ni.2524.

64. Nakamura M, Gotoh T, Okuno Y, et al. Activation of the endoplasmic reticulum stress pathway is associated with survival of myeloma cells. *Leuk Lymphoma*. 2006;47(3):531-539. doi:10.1080/10428190500312196.

65. Hoang B, Benavides A, Shi Y, Frost P, Lichtenstein A. Effect of autophagy on multiple myeloma cell viability. *Mol Cancer Ther*. 2009;8(7):1974-1984. doi:10.1158/1535-7163.MCT-08-1177.

66. Yun Z, Qun S. Targeting autophagy in multiple myeloma. *Leuk Res*. 2017;59(155):97-104. doi:10.1016/j.leukres.2017.06.002.

67. Bagratuni T, Wu P, Gonzalez de Castro D, et al. XBP1s levels are implicated in the biology and outcome of myeloma mediating different clinical outcomes to thalidomide-based treatments. *Blood*. 2010;116(2):250-253. doi:10.1182/blood-2010-01-263236.

68. Chhabra S, Jain S, Wallace C, Hong F, Liu B. High expression of endoplasmic reticulum chaperone grp94 is a novel molecular hallmark of malignant plasma cells in multiple myeloma. *J Hematol Oncol*. 2015;8(1):1-9. doi:10.1186/s13045-015-0177-6.

69. Travers KJ, Patil CK, Wodicka L, Lockhart DJ, Weissman JS, Walter P. Functional and Genomic Analyses Reveal an Essential Coordination between the Unfolded Protein Response and ER-Associated Degradation. *Cell*. 2000;101(3):249-258. doi:10.1016/S0092-8674(00)80835-1.

70. Coutu DL, Kokkaliaris KD, Kunz L, Schroeder T. Three-dimensional map of nonhematopoietic bone and bone-marrow cells and molecules. *Nat Biotechnol*. 2017;35(12):1202-1210. doi:10.1038/nbt.4006.

71. Tancred TM, Belch AR, Reiman T, Pilarski LM, Kirshner J. Altered expression of fibronectin and collagens I and IV in multiple myeloma and monoclonal gammopathy of undetermined significance. *J Histochem Cytochem*. 2009;57(3):239-247. doi:10.1369/jhc.2008.952200.

72. Terpos E, Dimopoulos MA, Sezer O, et al. The use of biochemical markers of bone remodeling in multiple myeloma: a report of the International Myeloma Working Group. *Leukemia*. 2010;24(10):1700-1712. doi:10.1038/leu.2010.173.

73. Avet-Loiseau H, Attal M, Moreau P, et al. Genetic abnormalities and survival in multiple myeloma: the experience of the Intergroupe Francophone du Myelome. *Blood*. 2007;109(8):3489-3495. doi:10.1182/blood-2006-08-040410.

74. Rajan AM, Rajkumar S V. Interpretation of cytogenetic results in multiple myeloma for clinical practice. *Blood Cancer J*. 2015;5(10):1-7. doi:10.1038/bcj.2015.92.

75. Fei M, Hang Q, Hou S, He S, Ruan C. Adhesion to fibronectin induces p27Kip1 nuclear accumulation through down-regulation of Jab1 and contributes to cell adhesion-mediated drug resistance (CAM-DR) in RPMI 8,226 cells. *Mol Cell Biochem*. 2014;386(1-2):177-187. doi:10.1007/s11010-013-1856-7.

76. Skliris A, Labropoulou VT, Papachristou DJ, Aletras A, Karamanos NK, Theocharis AD. Cell-surface serglycin promotes adhesion of myeloma cells to collagen type I and affects the expression of matrix metalloproteinases. *FEBS J*. 2013;280(10):2342-2352. doi:10.1111/febs.12179.

77. Kibler C, Schermutzkp F, Waller HD, Timpl R, Klein G. Adhesive Interactions of Human Multiple Myeloma Cell Lines with Different Extracellular Matrix Molecules. *Cell Adhes Commun*. 1998;5(4):307-323. doi:10.3109/15419069809040300.

78. Wajs J, Sawicki W. The morphology of myeloma cells changes with progression of the disease. *Wspolczesna Onkol*. 2013;17(3):272-275. doi:10.5114/wo.2013.35282.

79. Banerjee SS, Verma S, Shanks JH. Morphological variants of plasma cell tumours. *Histopathology*. 2004;44(1):2-8. doi:10.1111/j.1365-2559.2004.01763.x.

80. Ribourtout B, Zandecki M. Plasma cell morphology in multiple myeloma and related disorders. *Morphologie*. 2015;99(325):38-62. doi:10.1016/j.morpho.2015.02.001.

81. Ogata M, Hino S -i., Saito A, et al. Autophagy Is Activated for Cell Survival after Endoplasmic Reticulum Stress. *Mol Cell Biol*. 2006;26(24):9220-9231. doi:10.1128/MCB.01453-06.

82. Kouroku Y, Fujita E, Tanida I, et al. ER stress (PERK/eIF2α phosphorylation) mediates the polyglutamine-induced LC3 conversion, an essential step for autophagy formation. *Cell Death Differ*. 2007;14(2):230-239. doi:10.1038/sj.cdd.4401984.

83. White E. Deconvoluting the context-dependent role for autophagy in cancer. *Nat Rev Cancer*. 2012;12(6):401-410. doi:10.1038/nrc3262.

84. Carroll RG, Martin SJ. Autophagy in Multiple Myeloma: What Makes You Stronger Can Also Kill You. *Cancer Cell*. 2013;23(4):425-426. doi:10.1016/j.ccr.2013.04.001.

85. Robak P, Drozdz I, Szemraj J, Robak T. Drug resistance in multiple myeloma. *Cancer Treat Rev*. 2018;70(May 2018):199-208. doi:10.1016/j.ctrv.2018.09.001.

86. Manier S, Sacco A, Leleu X, Ghobrial IM, Roccaro AM. Bone marrow microenvironment in multiple myeloma progression. *J Biomed Biotechnol*. 2012;2012. doi:10.1155/2012/157496.

87. Basak G, Srivastava A, Malhotra R, Carrier E. Multiple Myeloma Bone Marrow Niche. *Curr Pharm Biotechnol*. 2009;10(3):335-346. doi:10.2174/138920109787847493.

88. Méndez-Ferrer S, Michurina T V., Ferraro F, et al. Mesenchymal and haematopoietic stem cells form a unique bone marrow niche. *Nature*. 2010;466(7308):829-834. doi:10.1038/nature09262.

89. Zdzisińska B, Roliński J, Piersiak T, Kandefer-Szerszeń M. A comparison of cytokine production in 2-dimensional and 3-dimensional cultures of bone marrow stromal cells of muliple myeloma patients in response to RPMI8226 myeloma cells. *Folia Histochem Cytobiol*. 2009;47(1):69-74. doi:10.2478/v10042-009-0015-1.

90. Ferrarini M, Steimberg N, Ponzoni M, et al. Ex-Vivo Dynamic 3-D Culture of Human Tissues in the RCCS™ Bioreactor Allows the Study of Multiple Myeloma Biology and Response to Therapy. *PLoS One*. 2013;8(8):1-10. doi:10.1371/journal.pone.0071613.

91. Zhang W, Lee WY, Siegel DS, Tolias P, Zilberberg J. Patient-Specific 3D Microfluidic Tissue Model for Multiple Myeloma. *Tissue Eng Part C Methods*. 2014;20(8):663-670. doi:10.1089/ten.tec.2013.0490.

92. de la Puente P, Muz B, Gilson RC, et al. 3D tissue-engineered bone marrow as a novel model to study pathophysiology and drug resistance in multiple myeloma. *Biomaterials*. 2015;73(1):70-84. doi:10.1016/j.biomaterials.2015.09.017.

93. Valarmathi MT, Yost MJ, Goodwin RL, Potts JD. A Three-Dimensional Tubular Scaffold that Modulates the Osteogenic and Vasculogenic Differentiation of Rat Bone Marrow Stromal Cells. *Tissue Eng Part A*. 2008;14(4):491-504. doi:10.1089/tea.2007.0235.

94. Valarmathi MT, Goodwin RL, Fuseler JW, Davis JM, Yost MJ, Potts JD. A 3-D cardiac muscle construct for exploring adult marrow stem cell based myocardial regeneration. *Biomaterials*. 2010;31(12):3185-3200. doi:10.1016/j.biomaterials.2010.01.041.

95. Evans HJ, Price RL, Goodwin RL, Yost M, Sweet JK. Novel 3D culture system for study of cardiac myocyte development. *Am J Physiol Circ Physiol*. 2015;285(2):H570-H578. doi:10.1152/ajpheart.01027.2002.

96. Yost MJ, Baicu CF, Stonerock CE, et al. A Novel Tubular Scaffold for Cardiovascular Tissue Engineering. *Tissue Eng*. 2004;10(1/2):273-287.

97. Jones RS, Chang PH, Perahia T, et al. Design and Fabrication of a Three-Dimensional in Vitro System for Modeling Vascular Stenosis. *Microsc Microanal*. 2017;23(4):859-871. doi:10.1017/S1431927617012302.

98. Lane BA, Harmon KA, Goodwin RL, Yost MJ, Shazly T, Eberth JF. Constitutive modeling of compressible type-I collagen hydrogels. *Med Eng Phys*. 2018;53:39-48. doi:10.1016/j.medengphy.2018.01.003.

99. Harmon KA, Lane BA, Boone RE, et al. Therapeutic Engineered Hydrogel Coatings Attenuate the Foreign Body Response in Submuscular Implants. *Ann Plast Surg*. April 2018:1. doi:10.1097/SAP.0000000000001347.

100. Gupta VA, Matulis SM, Conage-Pough JE, et al. Bone marrow microenvironment–derived signals induce Mcl-1 dependence in multiple myeloma. *Blood*. 2017;129(14):1969-1979. doi:10.1182/blood-2016-10-745059.

101. Gupta D, Treon SP, Shima Y, et al. Adherence of multiple myeloma cells to bone marrow stromal cells upregulates vascular endothelial growth factor secretion: therapeutic applications. *Leukemia*. 2001;15(12):1950-1961. doi:10.1038/sj.leu.2402295.

102. Landskron G, De la Fuente M, Thuwajit P, Thuwajit C, Hermoso MA. Chronic Inflammation and Cytokines in the Tumor Microenvironment. *J Immunol Res*. 2014;2014:1-19. doi:10.1155/2014/149185.

103. Nutt SL, Hodgkin PD, Tarlinton DM, Corcoran LM. The generation of antibody-secreting plasma cells. *Nat Rev Immunol*. 2015;15(3):160-171. doi:10.1038/nri3795.

104. Shapiro-Shelef M, Calame KC. Regulation of plasma-cell development. *Nat Rev Immunol*. 2005;5(3):230-242. doi:10.1038/nri1572.

105. Wang L, Jin FY, Li Y, et al. IgA Type Multiple Myeloma, Clinical Features, and Prognosis. *Chin Med J (Engl)*. 2018;131(10):1249-1250. doi:10.4103/0366-6999.231513.

106. Martinez-Murillo P, Pramanik L, Sundling C, et al. CD138 and CD31 double-positive cells comprise the functional antibody-secreting plasma cell compartment in primate bone marrow. *Front Immunol*. 2016;7(JUN):1-10. doi:10.3389/fimmu.2016.00242.

107. Jourdan M, Cren M, Robert N, et al. IL-6 supports the generation of human long-lived plasma cells in combination with either APRIL or stromal cell-soluble factors. *Leukemia*. 2014;28(8):1647-1656. doi:10.1038/leu.2014.61.

108. Winter O, Dame C, Jundt F, Hiepe F. Pathogenic Long-Lived Plasma Cells and Their Survival Niches in Autoimmunity, Malignancy, and Allergy. *J Immunol*. 2012;189(11):5105-5111. doi:10.4049/jimmunol.1202317.

109. Nutt SL, Hodgkin PD, Tarlinton DM, Corcoran LM. The generation of antibody-secreting plasma cells. *Nat Rev Immunol*. 2015;15(3):160-171. doi:10.1038/nri3795.

110. DiEgidio P, Friedman HI, Gourdie RG, Riley AE, Yost MJ, Goodwin RL. Biomedical Implant Capsule Formation: Lessons Learned and the Road Ahead. *Ann Plast Surg*. 2014;00(4):1-10. doi:10.1097/SAP.0000000000000287.

111. Major MR, Wong VW, Nelson ER, Longaker MT, Gurtner GC. The Foreign Body Response. *Plast Reconstr Surg*. 2015;135(5):1489-1498. doi:10.1097/PRS.0000000000001193.

112. Vishwakarma A, Bhise NS, Evangelista MB, et al. Engineering Immunomodulatory Biomaterials To Tune the Inflammatory Response. *Trends Biotechnol*. 2016;34(6):470-482. doi:10.1016/j.tibtech.2016.03.009.

113. Sheikh Z, Brooks PJ, Barzilay O, Fine N, Glogauer M. Macrophages, foreign body giant cells and their response to implantable biomaterials. *Materials (Basel)*. 2015;8(9). doi:10.3390/ma8095269.

114. Wynn TA, Vannella KM. Macrophages in Tissue Repair, Regeneration, and Fibrosis. *Immunity*. 2016;44(3). doi:10.1016/j.immuni.2016.02.015.

115. Mescher AL. Macrophages and fibroblasts during inflammation and tissue repair in models of organ regeneration. *Regeneration*. 2017;4(2):39-53. doi:10.1002/reg2.77.

116. Kyriakides TR, Foster MJ, Keeney GE, et al. The CC chemokine ligand, CCL2/MCP1, participates in macrophage fusion and foreign body giant cell formation. *Am J Pathol*. 2004;165(6):2157-2166. doi:10.1016/S0002-9440(10)63265-8.

117. Parker JATC, Walboomers XF, Von Den Hoff JW, Maltha JC, Jansen JA. Soft tissue response to microtextured silicone and poly-L-lactic acid implants: Fibronectin pre-coating vs. radio-frequency glow discharge treatment. *Biomaterials*. 2002;23(17):3545-3553. doi:10.1016/S0142-9612(02)00033-9.

118. Moreira M, Fagundes DJ, De Jesus Simoes M, Taha MO, Perez LMN, Bazotte RB. The effect of liposome-delivered prednisolone on collagen density, myofibroblasts, and fibrous capsule thickness around silicone breast implants in rats. *Wound Repair Regen*. 2010;18(4):417-425. doi:10.1111/j.1524-475X.2010.00601.x.

119. Bastos EM, Neto MS, Alves MTS, et al. Histologic analysis of zafirlukast's effect on capsule formation around silicone implants. *Aesthetic Plast Surg*. 2007;31(5):559-565. doi:10.1007/s00266-006-0257-7.

120. Zhang L, Cao Z, Bai T, et al. Zwitterionic hydrogels implanted in mice resist the foreign-body reaction. *Nat Biotechnol*. 2013;31(6):553-556. doi:10.1038/nbt.2580.

121. Soder BL, Propst JT, Brooks TM, et al. The connexin43 carboxyl-terminal peptide ACT1 modulates the biological response to silicone implants. *Plast Reconstr Surg*. 2009;123:1440-1451. doi:10.1097/PRS.0b013e3181a0741d.

122. Friedman H, Stonerock C, Lefaivre J, Yost M. The effect of seprafilm and interceed on capsule formation around silicone discs in a rat model. *J Invest Surg*. 2004;17:271-281. doi:10.1080/08941930490502844.

123. Friedman HI, Giurgiutiu V, Bender J, Crachiolo G, Yost MJ. A biomechanical and morphologic analysis of capsule formation around implanted piezoelectric wafer active sensors in rats treated with cyclooxygenase-2 inhibition. *Ann Plast Surg*. 2008;60(2):198-203. doi:10.1097/SAP.0b013e3180546963.

124. Dalbeth N, Lauterio TJ, Wolfe HR. Mechanism of Action of Colchicine in the Treatment of Gout. *Clin Ther*. 2014;36(10):1465-1479.

125. Acuner B, Baser NT, Aslan G, et al. The Effects of Colchicine-Impregnated Oxidized Regenerated Cellulose on Capsular Contracture. *Surg Innov*. 2017:155335061771891. doi:10.1177/1553350617718915.

126. Kaur M, Singh D. Neutrophil Chemotaxis Caused by Chronic Obstructive Pulmonary Disease Alveolar Macrophages : The Role of CXCL8 and the Receptors CXCR1 / CXCR2. *J Pharmacol Exp Ther*. 2013;(347):173-180.

127. Powell D, Tauzin S, Hind LE, Deng Q, Beebe DJ, Huttenlocher A. Chemokine Signaling and the Regulation of Bidirectional Leukocyte Migration in Interstitial Tissues. *Cell Rep*. 2017;19(8):1572-1585. doi:10.1016/j.celrep.2017.04.078.

128. Caratti G, Matthews L, Poolman T, Kershaw S, Baxter M, Ray D. Glucocorticoid receptor function in health and disease. *Clin Endocrinol (Oxf)*. 2015;83(4):441-448. doi:10.1111/cen.12728.

129. Vacanti NM, Cheng H, Hill PS, et al. Localized delivery of dexamethasone from electrospun fibers reduces the foreign body response. *Biomacromolecules*. 2012;13(10):3031-3038. doi:10.1021/bm300520u.

130. Acarregui A, Herrán E, Igartua M, et al. Multifunctional hydrogel-based scaffold for improving the functionality of encapsulated therapeutic cells and reducing inflammatory response. *Acta Biomater*. 2014;10(10):4206-4216. doi:10.1016/j.actbio.2014.06.038.

131. Kastellorizios M, Papadimitrakopoulos F, Burgess DJ. Multiple tissue response modifiers to promote angiogenesis and prevent the foreign body reaction around subcutaneous implants. *J Control Release*. 2015;214:103-111. doi:10.1016/j.jconrel.2015.07.021.

132. Charo IF, Ransohoff RM. The Many Roles of Chemokines and Chemokine Receptors in Inflammation. *N Engl J Med*. 2006;354(6):610-621. doi:10.1056/NEJMra052723.

133. Jones JA, Chang DT, Meyerson H, et al. Proteomic analysis and quantification of cytokines and chemokines from biomaterial surface-adherent macrophages and foreign body giant cells. *J Biomed Mater Res Part A*. 2007;83A(3):585-596. doi:10.1002/jbm.a.

134. Rodriguez A, Meyerson H, Anderson JM. Quantitative in vivo Cytokine Analysis at Synthetic Biomaterial Implant Sites. *J Biomed Mater Res*. 2009;89(1). doi:10.1007/s11103-011-9767-z.Plastid.

APPENDIX A[1]

THERAPEUTIC ENGINEERED HYDROGEL COATINGS ATTENUATE THE FOREIGN BODY RESPONSE IN SUBMUSCULAR IMPLANTS

[1]Harmon KA, Lane BA, Boone RE, et al. Therapeutic Engineered Hydrogel Coatings Attenuate the Foreign Body Response in Submuscular Implants. *Annals of Plastic Surgery*. 2018;80. doi:10.1097/sap.0000000000001347.

A.1 Abstract

Background: Biomedical devices are implanted into mammalian soft tissues to improve, monitor, or restore form or function. The utility of these implants is limited by the subsequent foreign body response (FBR), beginning with inflammation and terminating in a collagen envelope around the device, known as the capsule. This capsule then can contract and distort the shape of the device or limit its effectiveness in interacting with the surrounding host tissues. In the current study, we investigated the effect of therapeutic collagen-coated silicone discs in a rat model of the FBR.

Methods: A 3-dimensional printed mold was used to fabricate collagen-coated silicone discs incorporating 3 therapeutic agents: colchicine, a function-blocking antibody against interleukin 8 (IL-8) receptor B, and a powerful anti-inflammatory steroid, dexamethasone. Discs were implanted submuscularly into a well characterized rat model of the FBR and evaluated for inflammatory response, fibrotic development, and cytokine release.

Results: Coated silicone discs exhibited reduced collagen deposition and little to no foreign body giant cells at the host-silicone interface when compared with the silicone-only group. Therapeutic hydrogels demonstrate a significant decrease in cellular infiltration into the coatings over the 2-week time point in contrast to therapeutic-free hydrogel coatings. Cytokine analysis revealed significant differences between therapeutic-free and therapeutic-containing coatings when

compared with silicone-only controls. Levels of IL-1β, IL-6, monocyte chemotactic protein 1, and macrophage inflammatory protein 3α were affected 48 hours after implantation, while differences in IL-18, growth- regulated oncogene/keratinocyte chemoattractant, and macrophage inflammatory protein 3α were observed 1 week after implantation.

Conclusions: By utilizing the host's innate immune response, our engineered hydrogel coatings delivered therapeutic moieties directly to the implant microenvironment, thus delaying the FBR up to 2 weeks.

Key Words: drug elution, foreign body reaction, hydrogel coatings, implant capsule, implant fibrosis.

A.2 Introduction

Biomedical devices are designed to improve or restore form and/or function through interactions with native tissue. The utility of these devices is limited by the foreign body response (FBR). Initially, there is a peri-implant inflammation that is eventually encapsulated in a dense connective tissue layer composed primarily of type I collagen. The FBR is implicated in implant malfunction and failure by inhibiting the device from responding to the local microenvironment or deforming the shape of the implant. The FBR is a modified wound healing response that has been well characterized and reviewed elsewhere. Briefly, cellular debris and platelet aggregation on the surface of the implant trigger an initial inflammatory

reaction, recruiting neutrophils and macrophages to the implant surface via intercellular signaling.[110–112] Activated macrophages at the implant surface undergo fusion to form multinucleated giant cells.[113–115] These foreign body giant cells are present at the tissue-implant interface and are unique to the FBR.[116] Cytokines produced by neutrophils and macrophages signal fibroblast migration onto the surface where they begin deposition of collagenous extracellular matrix around the implant, effectively walling it off from host tissue.[115] Fibroblasts frequently differentiate into myofibroblasts, which mediate capsule contraction, further distorting the implant.[110,111]

Research regarding peri-implant fibrosis has focused on topographical changes to the implant, systemic and local administration of drugs, and coating implants in biomaterials.[110] Thus far, techniques aimed to prevent fibrotic capsule formation have temporarily delayed the FBR. Physical modifications to the implant include the investigation of smooth versus textured implants,[117] changes in implant thickness, and changes in implant composition. However, these alterations have had minimal effects on ultimate capsule formation.[1] Systemic administration of drugs shown to inhibit inflammation and wound healing has not influenced capsule formation or contraction.[118–120] Similarly, the administration of drugs that affect cellular responses occurring during the FBR is ineffective or too toxic at efficacious levels. Therefore, we and others have used therapeutic agents and biomaterials to loosely coat implants to improve the local microenvironment and resulting inflammation and fibrosis.[121–123] Although a temporary delay of fibrosis has been seen, no single method has completely eliminated capsule formation, suggesting

that a multifactorial approach, with a variety of different inflammatory inhibiting chemical moieties and physical properties, offers the greatest opportunity to provide an improved host microenvironment.

Implanted devices create a procoagulatory, proadhesive, and proinflammatory microenvironment in host soft tissues. Consequently, there is little opportunity to intervene in the early stages of the innate immune response. For this reason, we have chosen to target the next steps of the FBR, focusing on cell recruitment, proliferation, and differentiation at the implant site and the beginning of pathological remodeling proteases, including those that degrade extracellular matrix molecules. We elected to coat biomedical implants with a hydrogel coating composed of type I collagen, which would allow host collagenases to degrade the implant coating, thereby releasing the therapeutic agents incorporated within the hydrogel.

Here, we report the fabrication of implants coated with a degradable, therapeutic biomaterial to control host responses, with the goal of improving implant function and the local microenvironment. Numerous therapeutics can be incorporated into our hydrogel coating including small molecules, antibodies, and steroids. A well-characterized rat model of the FBR was used to submuscularly implant silicone discs coated in the therapeutic hydrogel containing 3 agents.[123] First, colchicine, clinically used to treat gout, has been shown to inhibit microtubule formation while reducing the migration and proliferation of inflammatory cells.[124,125] Next, an antibody against interleukin 8 receptor B (anti–IL-8), which has been previously reported to limit neutrophil activation and recruitment.[126,127] Lastly,

dexamethasone, a powerful corticosteroid, is clinically used to limit inflammation by modulation of the steroid response transcriptional network, thus preventing the release of cytokines that cause inflammation.[128–131] Dexamethasone interferes with collagen formation further by preventing excessive scar tissue formation. In this investigation, we used these 3 moieties, both alone and in combination, to elucidate their effect on the early inflammatory response.

A.3 Materials and Methods

Hydrogel Fabrication

Bovine type I collagen was isolated using methods previously described in Yost et al.[96] Briefly, isolated bovine dermis was acid solubilized and pepsin digested to an average concentration of 3.12% (dry weight/wet weight), which was sterilized with 1200 rad γ-irradiation prior to fabrication. Therapeutic agents were added to the collagen at final concentrations of colchicine at 40 μg/mL (Fisher Scientific, Pittsburgh, Pa), anti–IL-8 at 833 μg/mL (R&D Systems, Minneapolis, Minn), and dexamethasone at 350 μg/mL (Sigma, St Louis, Mo). Silicone-only and therapeutic-free–coated controls were also used in these experiments.

A 3-dimensional polylactic acid mold was used to fabricate collagen-coated silicone discs (Figure. A.1). The therapeutic or therapeutic-free collagen mixture was syringed into the 3-dimensional printed mold, and a sterile 8-mm silicone disc was placed into the center, creating a 1-mm hydrogel coating around the silicone, as depicted in Figures A.1 B and C. Hydrogels were polymerized with 10X HEPES

buffer at pH 7.8 for 1 hour. Polymerized hydrogel discs were then exposed to 10^7μJ of UV crosslinking, per side, prior to implantation.

Experimental Animals

Sprague-Dawley rats were maintained at the Department of Laboratory Animal Resources, University of South Carolina. The number of animals used within this study was kept to a minimum, and all possible efforts were made to reduce suffering in compliance with the protocols established by the Institutional Animal Care and Use Committee of the University of South Carolina. Our experimental protocol was approved by the Institutional Animal Care and Use Committee (AUP #2322).

For histological analysis, silicone-only, collagen-only, colchicine + anti–IL-8, and dexamethasone + anti–IL-8 coatings were fabricated and placed into a pocket created beneath the aponeurosis of the trapezius muscles, with 1 disc being placed in each animal. Discs and the surrounding tissue were harvested at 48 hours, 1 week, and 2 weeks after implantation. For cytokine analysis, treatment groups included silicone-only controls, collagen-only, anti–IL-8, dexamethasone, and dexamethasone + anti–IL-8 coatings. These discs were also placed in the submuscular pocket and were collected 48 hours and 1 week after implantation.

Histological Assessment of Cellular Invasion

Tissue samples collected for histology were fixed, paraffin embedded, sectioned, and processed for light microscopy. Masson trichrome stain was used

to identify cell invasion, collagen remodeling, collagen deposition, and the presence of foreign body giant cells. Additional sections stained with hematoxylin-eosin were used to investigate inflammatory cell invasion via blinded examiners. Morphometric analysis of the remodeling process that occurs in the coatings and surrounding tissue was quantified via the National Institutes of Health ImageJ by determining cellular density in 3 different zones of the surrounding tissue and hydrogel coating. Zones designated for analysis include host tissue-hydrogel interface (THI), hydrogel (H), and silicone-hydrogel interface (SHI).

Cytokine Processing

A 5-mm^3 section from the harvested implants and surrounding tissue was frozen at −80°C. Samples were thawed, and cell lysis was carried out according to the Bio-Plex Cell Lysis Kit protocol (Bio-Rad Laboratories, Hercules, Calif). Briefly, tissue samples were washed, and lysing solution was added. Tissues were homogenized prior to being frozen at −80°C. Thawed samples were sonicated and centrifuged, and supernatants were collected. Lysates were diluted to a final concentration of 800 µg/mL.

Sample lysates were analyzed according to the Bio-Plex Rat Cytokine Group I (Bio-Rad Laboratories) protocol to determine differences in inflammatory cytokine levels between silicone-only and therapeutic and nontherapeutic hydrogels.

Statistical Analysis

Statistical significance to evaluate cellular infiltration into the hydrogel was determined by 2-way analysis of variance and Tukey multiple-comparisons test. Cytokine analysis was determined by 1-way analysis of variance and Bonferroni multiple-comparisons test with α values of 0.05. Differences between groups were considered significant with $P < 0.05$.

A.4 Results

Characterization of Polymerized Hydrogels

In order to characterize the microarchitecture of our hydrogel coatings, scanning electron microscopy was carried out on therapeutic-free hydrogels, without a silicone disc. As seen in Figure A.2, the collagen solution polymerizes into microfibrils that are less than 1 μm in diameter. Higher magnification demonstrates that these fibrils form an anisotropic network of collagen, which is capable of incorporating a wide range of therapeutic molecules, while being biocompatible (Figure. A.2C).

Silicone-Only Implants

To demonstrate the progression of the FBR in our model system, uncoated silicone discs were placed under the aponeurosis of the trapezius muscle. The size and submuscular placement of the silicone disc were to model the FBR that occurs in the commonly performed sub-pectoral breast implant procedure. Figure A.3 shows stained Masson trichrome at 1 and 2 weeks after implantation. Images

exhibit infiltration of inflammatory cells to the site of the implant and layers of fibrous connective tissues around the implant surface. In addition, 2-week images show numerous multinucleated foreign body giant cells lining the silicone disc at the host-implant interface (red arrow, Figure. A.3B).

Therapeutic-Free and Therapeutic Hydrogel Coatings

To determine the effect of therapeutic combinations in our model systems, therapeutic-free and therapeutic hydrogel coatings were submuscularly implanted. Implants and the surrounding tissues were then collected 48 hours, 1 week, and 2 weeks after implantation for histological analysis. Therapeutic-free coatings 48 hours after implantation displayed inflammatory cell infiltration, with most cells located at the host THI, and limited collagen remodeling (Figure. A.4A). Less cellular infiltration was observed in hydrogel coatings containing a combination of colchicine + anti–IL-8 and dexamethasone + anti–IL-8 (Figures. A.4B, C). In addition, fewer cells are located at this host-implant interface when compared with therapeutic-free hydrogels. By 1 week, collagen-only coatings demonstrate increased cell invasion into the hydrogel coating, with cells being distributed throughout the collagen as opposed to being primarily located at the THI (Figure. A.5A). Remodeling of the hydrogel coatings has also begun as robust collagen staining (blue) is observed at the silicone interface. Colchicine + anti–IL-8 and dexamethasone + anti–IL-8 have limited cellular invasion, with cells clustering at the THI (Figures. A.5B, C). Minimal collagen remodeling was observed in therapeutic-containing coatings, and little to no collagen was evident. Two weeks

after implantation, therapeutic-free hydrogels exhibited the advanced stages of the FBR including massive cellular infiltration throughout the coating and increased collagen remodeling, with collagen deposition at the silicone interface (Figure. A.6A). Colchicine + anti–IL-8 coatings show a slight increase in collagen remodeling and cellular infiltration into the hydrogel; however, fewer cells are present when compared with collagen-only controls (Figure. A.6B). While some collagen remodeling has occurred in dexamethasone + anti–IL-8 hydrogels, cellular infiltration remains low when compared with other coatings (Figure. A.6C).

Morphometric Analysis of Cellular Invasion

Sections were stained with hematoxylin-eosin, imaged, and analyzed to determine cellular density in 3 regions of the hydrogel coatings. Figure A.7 depicts the zones identified for analysis including THI, H, and SHI. Therapeutic-free coatings, 48 hours after implantation, show most cells localized at the THI, with some cells located in the H and SHI. Both combinations (colchicine + anti–IL-8 and dexamethasone + anti–IL-8) of therapeutic hydrogels revealed a significant decrease in inflammatory cell infiltration at the THI when compared with therapeutic-free controls. In addition, colchicine + anti–IL-8 coatings exhibit a significant reduction in cells present at the SHI. By week 1, controls display an increased number of cells found at the THI. Therapeutic-containing hydrogels significantly decreased cellular density at all 3 zones when compared with collagen-only implants. Additional analysis demonstrated significant differences at the 2-week time point within the THI and SHI zones for both treatments;

furthermore, the hydrogel zone was also significant for the dexamethasone + anti–IL-8 coating (Figure. A.8).

Inflammatory Cytokine Analysis

Lysates from the hydrogel disc and surrounding tissues were harvested to determine levels of cytokine expression, when compared with silicone-only controls, 48 hours and 1 week after implantation. Interleukin 1β and IL-6 were elevated in control lysates, 48 hours after implantation, whereas therapeutic-free and therapeutic-containing hydrogels expressed significantly lower levels (Figure. A.9). In addition, macrophage inflammatory protein 3α (MIP-3α) was decreased in all therapeutic-containing coatings, and monocyte chemotactic protein 1 (Figures. A.9, A.10) levels were decreased in anti–IL-8 and dexamethasone collagen hydrogels. By 1 week, expression levels of IL-18 were decreased in anti–IL-8 hydrogels when compared with silicone-only controls (Figure. 2.11). Growth-regulated oncogene/keratinocyte chemoattractant (GRO/KC) levels significantly increased in all therapeutic-containing coatings, and MIP-3α was elevated in anti–IL-8 coatings (Figure. A.11). Cytokine analysis also revealed that IL-1α, IL-10, interferon γ, and tumor necrosis factor α expression levels were not significantly affected by the collagen hydrogel coatings, with or without therapeutic moieties.

A.5 Discussion

The foreign body reaction is an irreversible process that occurs around biomedical implants, often providing detrimental consequences to the form and

function of the implant. Despite temporary delays of fibrosis, no single technique has eliminated implant encapsulation; hence, a multifactorial approach is needed to improve the host microenvironment.[110,112] A number of methodologies have been developed prior to this investigation; however, few have used the host's innate response to deliver therapeutic agents to the implant site.[118,119] While future studies involving further manipulation and analysis of the effects of the therapeutics are required, our model system presented provides an innovative method for gaining insight into implant fibrosis.

In our model, early and late visualization of the FBR has been studied; thus, we can predict the outcome, for up to 2 months, by examining the results at 2 weeks.[121] The rat FBR model system was validated by implanting silicone-only discs. This study found that uncoated silicone discs underwent classic progression of the FBR, which is a common clinical observation in sub-pectoral implant procedures. This is marked by cellular invasion, collagen deposition, and the formation of foreign body giant cells at the implant surface. The microarchitecture of our collagen coatings exhibited polymerized microfibrils in an anisotropic arrangement, mimicking irregular connective tissue. The hydrogel is biocompatible; however, the host's innate responses result in enzymatic activity that degrades the collagen, allowing for the release of therapeutic agents that are localized at the implant microenvironment. Therapeutic combinations (colchicine + anti–IL-8 and dexamethasone + anti–IL-8) delayed the FBR 2 weeks after implantation, when com- pared with collagen-only implants, with decreased cellular infiltration and collagen remodeling.

During the early progression of the FBR, macrophages are recruited to the implant surface via intercellular signaling. Interleukin 1β and IL-6 are proinflammatory cytokines that are produced and secreted by activated macrophages.[115] Expression levels for both IL-1β and IL-6 were significantly decreased in collagen-coated when compared with silicone-only controls. Furthermore, levels of cytokines known to recruit monocytes/macrophages during the fibrotic response, monocyte chemotactic protein 1 and MIP-3α, were also decreased, specifically in therapeutic coatings.[132] At 48 hours after implantation, these results suggest that fewer macrophages were recruited to the silicone implant site, thus indicating that the therapeutic moieties used delayed the FBR. By 1 week, decreased levels of IL-18 were exhibited in anti– IL-8 coatings, whereas levels of MIP-3α were significantly elevated. Growth-regulated oncogene/keratinocyte chemoattractant, a murine homolog to IL-8, is secreted by adherent macrophages and foreign body giant cells in vitro, which recruits neutrophils to the site of implantation.[132,133] The GRO/KC concentrations were significantly higher in therapeutic-containing collagen implants than in the control group. This may be due to surface adherent cells contributing to the production of GRO/KC.[134]

Our therapeutic moieties delayed the FBR response 2 weeks prior to coatings exhibiting the progression of the response, suggesting the eventuality of a complete reaction. The cytokine analysis of the implants may indicate that the therapeutic moieties were no longer efficacious in delaying the FBR, and the progression of the reaction continued beyond the 2-week time interval. The

moieties could have been absorbed by host tissues or may have undergone hydrolysis by host enzymes, thereby inhibiting their efficacy over the 2-week period. Dexamethasone is a powerful corticoid steroid that should have attenuated the FBR for an extended period, as previous studies have indicated.[130,131] Unfortunately, these hydrogels exhibited minimal cellular infiltration into the collagen, although they presented with limited collagen remodeling and little to no foreign body giant cells. The bioactivity of dexamethasone may have been compromised during the fabrication process, specifically UV crosslinking, which could have diminished its efficacy over the 2-week time point. Thus, further experimentation is necessary to effect of crosslinking on the activity of our moieties.

A.6 Conclusions

Using a unique fabrication approach that allows for the incorporation of various therapeutic agents into a hydrogel coating implanted into a well-characterized rat model, we have created an implant that delays and alters the FBR 2 weeks after implantation. The limitation of the model is the eventual dissipation or degradation of the drugs incorporated into the collagen. Future investigations involve utilizing all 3 therapeutic moieties, and others, in an attempt to elicit a sustained and regenerative response to the implantation of biomaterials. The complex cytokine signaling during the FBR has been extensively studied; however, the ability to drive this response away from a fibrotic scar and toward a

regenerative process has met with limited clinical success. Our hydrogel coating has the capability of incorporating small molecules and viable cells.

Finally, our model allows for the incorporation of viable cells, including stem cells, into the collagen matrix, which may provide a future direction for our research by influencing the behavior and activity of the inflammatory cells. Our fabrication process offers a substantial approach with extensive potential to contribute to the field of research for implant fibrosis.

Figure A.1. A schematic of the 3-dimensional polylactic acid mold (A) used to fabricate implants with uniform dimensions, creating an 8-mm silicone disc with a 1-mm collagen coating (B, C).

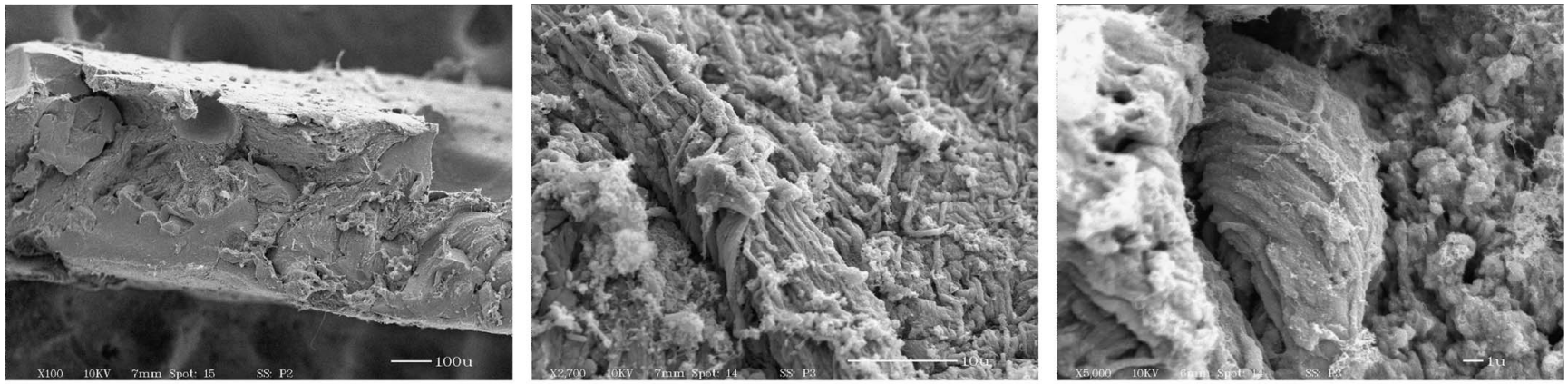

A B C

Figure A.2. Therapeutic-free hydrogels, without a silicone disc, demonstrate the microarchitecture of polymerized collagen, with microfibrils less than 1 μm in diameter. Increasing magnification shows an anisotropic fibril network, resembling collagen fibrils found in irregular dense connective tissue, confirming biocompatibility (original magnification ×100, ×2700, ×5000).

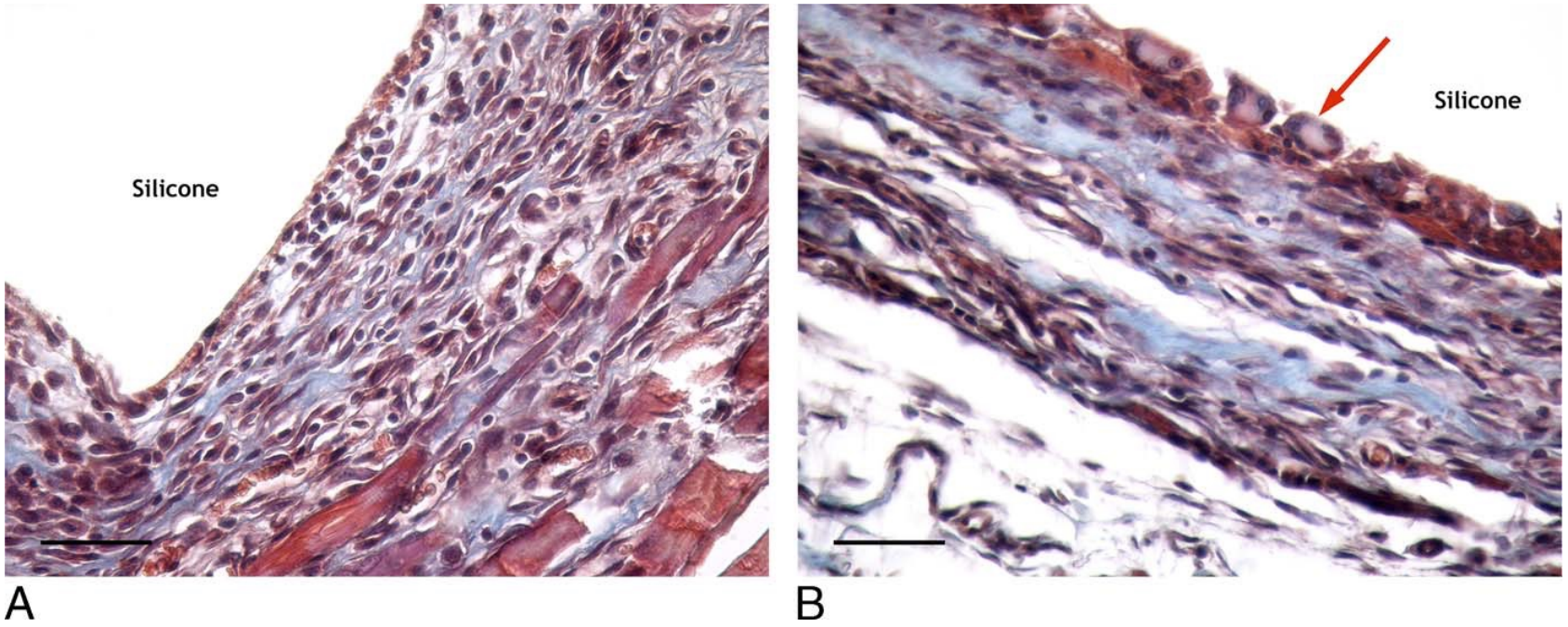

Figure A.3. Uncoated silicone discs implanted submuscularly displays the progression of the FBR within the rat model system. One week after implantation (A), layers of fibrous connective tissue have been deposited around the silicone implant, indicated by the blue stain. By 2 weeks (B), macrophages have undergone fusion to form multinucleated foreign body giant cells that line the implant surface (red arrow). Masson trichrome stain.

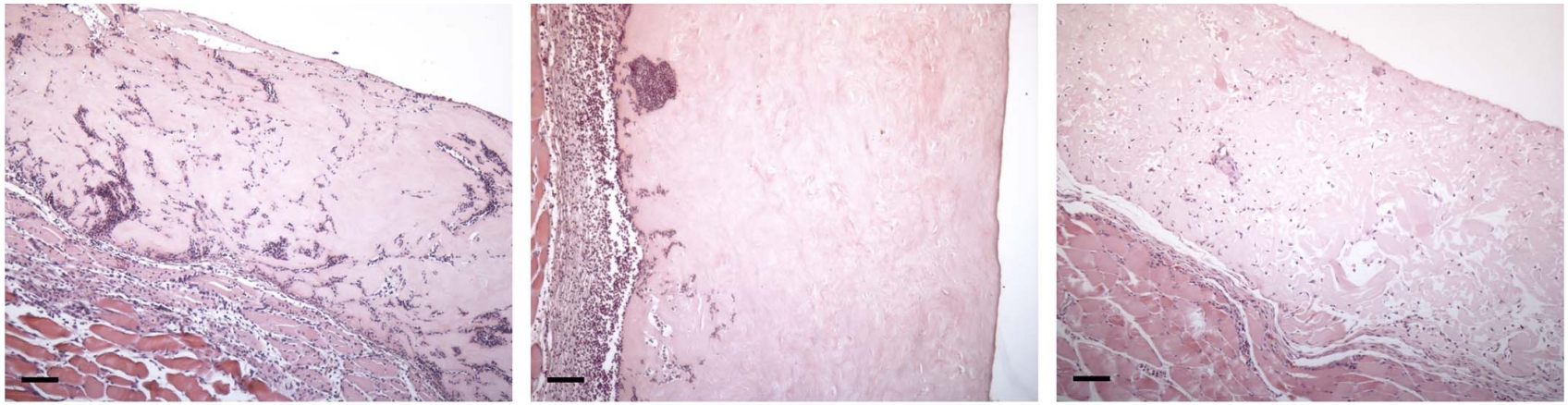

Figure A.4. Therapeutic-free collagen coatings (A), 48 hours after implantation, present with inflammatory cell infiltration into the hydrogel, and most cells are located at the THI. Less cell infiltration can be seen in colchicine + anti–IL-8 (B) and dexamethasone + anti–IL-8 (C) coatings.

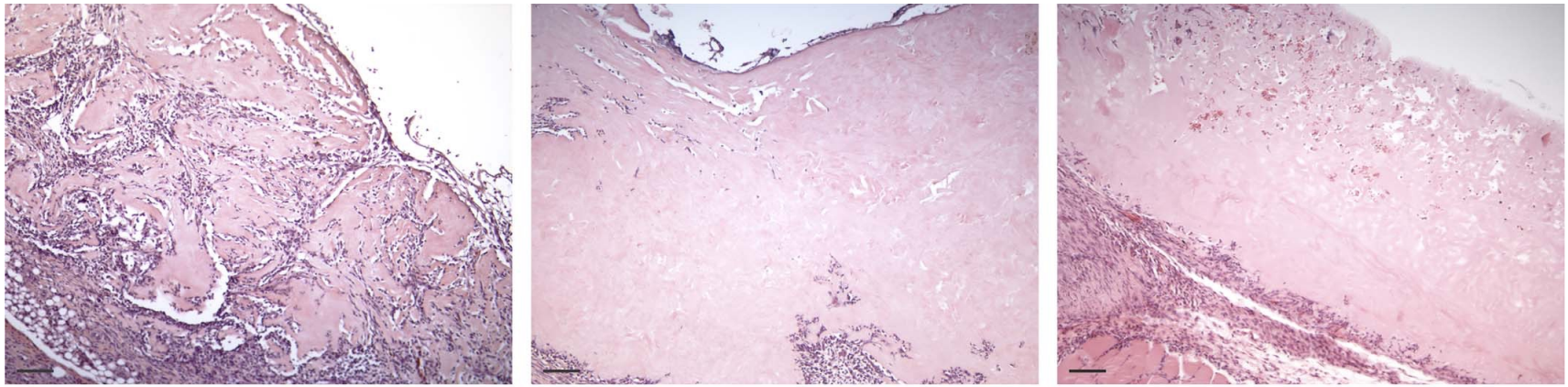

Figure A.5. One-week collagen coatings (A) demonstrate increased cellular invasion into the hydrogel, with cells being distributed throughout the collagen, and collagen remolding has begun. Colchicine + anti–IL-8 (B) and dexamethasone + anti–IL-8(C) therapeutic coatings have limited cell infiltration, and most cells are clustered at the THI. Minimal collagen remolding can be seen within these coatings.

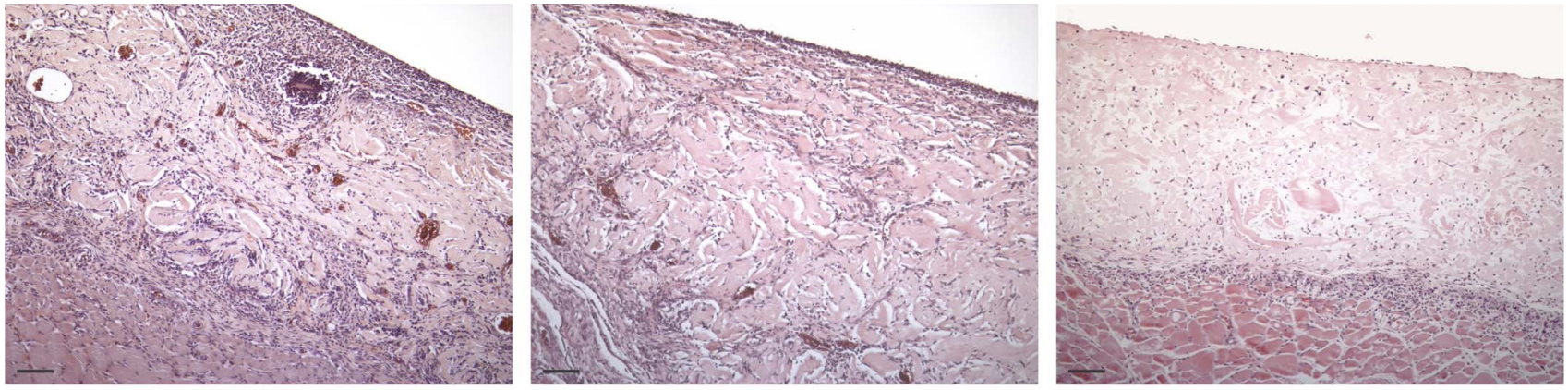

Figure A.6. Two weeks after implantation, collagen hydrogels (A) have massive cell infiltration within the coatings, and inflammatory cells are present at the SHI. New collagen deposition has begun at the silicone interface. Colchicine + anti–IL-8 (B) hydrogels exhibit a slight increase in cellular invasion; however, fewer cells are present at the SHI. Dexamethasone + anti–IL-8 (C) coatings have limited cellular infiltration when compared with other collagen coatings.

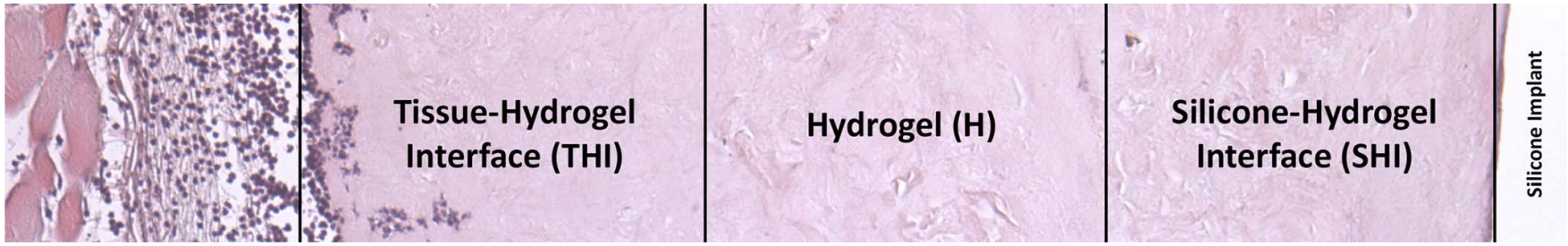

Figure A.7. Hematoxylin-eosin images were divided into 3 equal zones for morphometric analysis: THI, where host tissue encounters the implanted collagen coating, hydrogel interface (H) is consistent of collagen coating only, and SHI, where collagen coating meets the silicone implants.

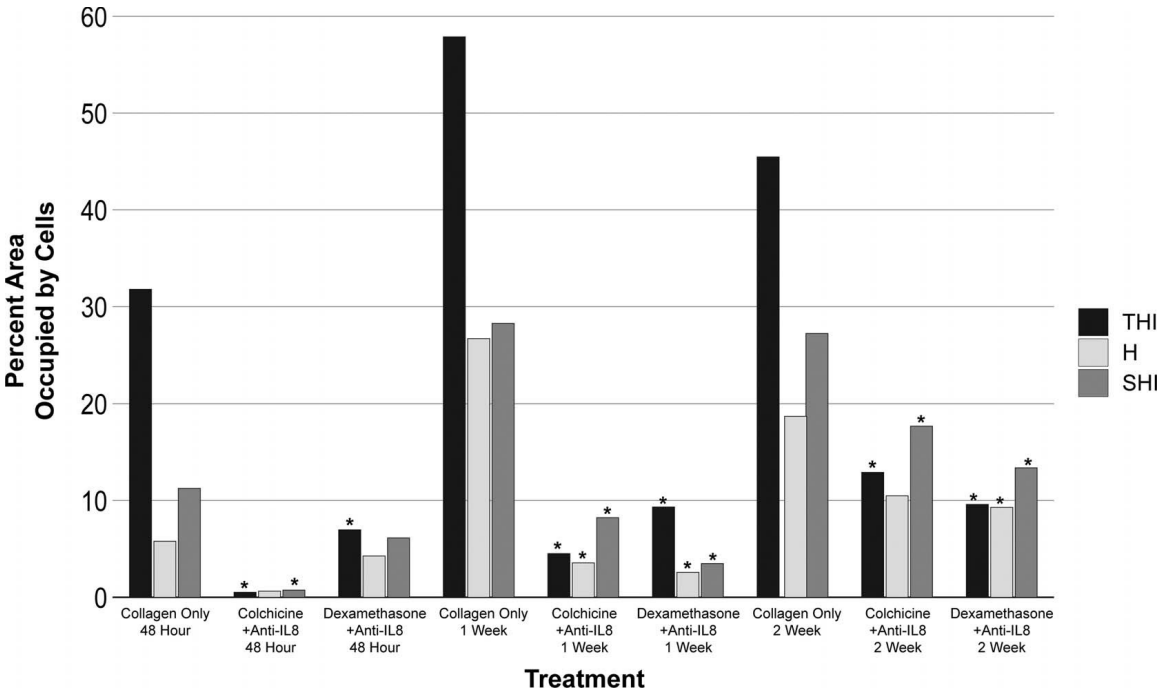

Figure A.8. Morphometric analysis of cellular infiltration into the collagen coating 48 hours, 1 week, and 2 weeks after implantation. When compared with collagen-only controls, colchicine + anti–IL-8 and dexamethasone + anti–IL-8 coatings present with significantly fewer cells within the THI 48 hours after implantation. By 1 week, hydrogel-only implants demonstrate an increase in cellular density within the coating. Therapeutic-containing hydrogels presented with a decrease in cellular density within the THI, H, and SHI interfaces. By 2 weeks, colchicine + anti–IL-8 and dexamethasone + anti–IL-8 collagen coatings continue to exhibit decreased cellular infiltration and the THI and SHI interfaces, when compared with collagen only coatings. In addition, dexamethasone + anti–IL-8 discs show a significant decrease at the hydrogel interface. Differences were considered significant with $P < 0.05$.

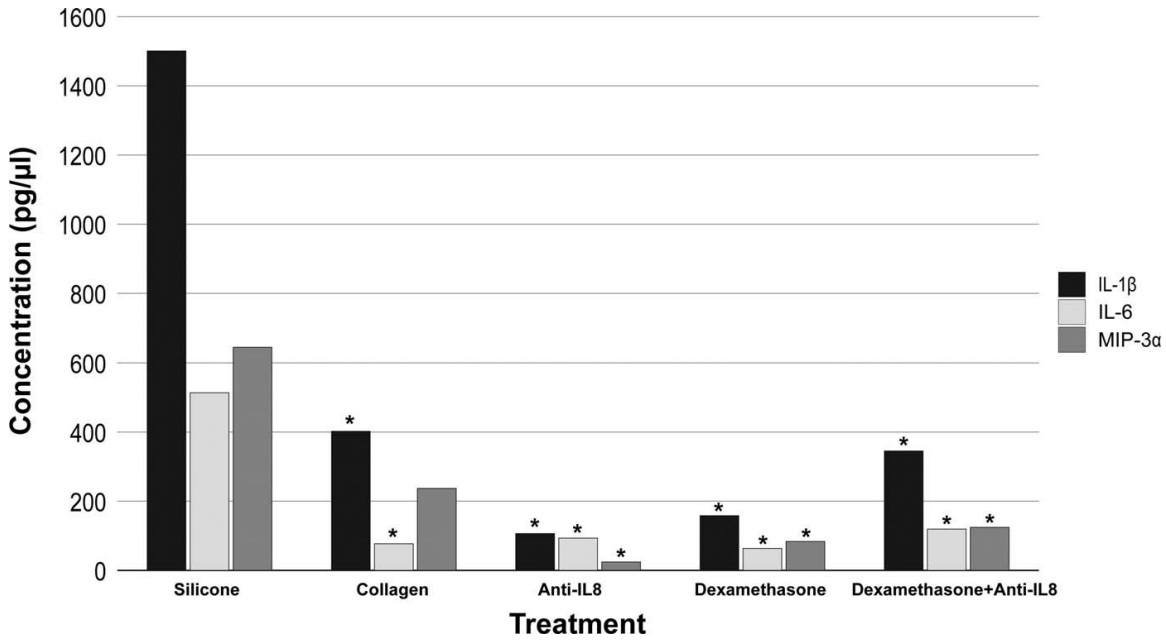

Figure A.9. Proinflammatory cytokines, IL-1β and IL-6, that are produced and secreted by activated macrophages exhibited decreased expression levels in all hydrogel coatings when compared with silicone-only controls, 48 hours after implantation. Expression levels of MIP-3α were significantly lower in therapeutic-containing coatings.

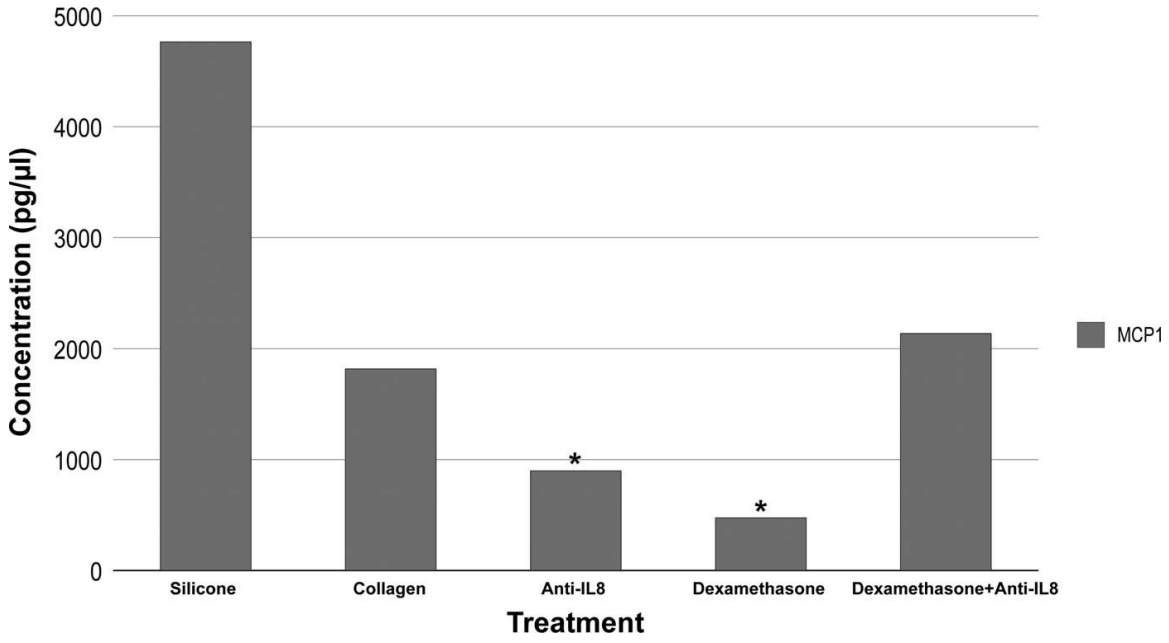

Figure A.10. Monocyte chemotactic protein 1, responsible for the recruitment of monocytes and macrophages during the fibrotic response, expression levels were significantly reduced in hydrogel coatings containing anti–IL-8 and dexamethasone coatings at 48 hours.

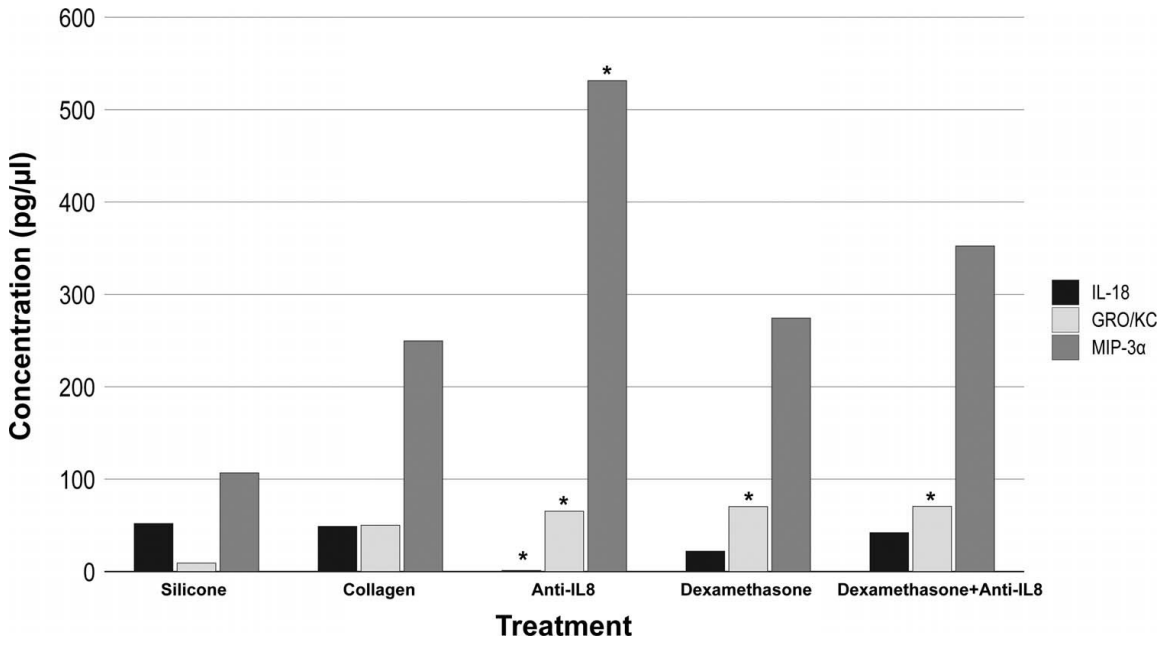

Figure A.11. By 1 week, decreased expression levels of IL-8 and increased levels of MIP-3α were exhibited in anti–IL-8 coatings when compared with silicone-only controls. Growth-regulated oncogene/keratinocyte chemoattractant demonstrated increased levels in therapeutic-containing coatings.

Figure A.12. Above is proof that Appendix A includes full-text that was reprinted with permission from a Wolters Kluwer Health, Inc. Journal, Annals of Plastic Surgery.